



HAL
open science

Light-wave propagation in Erbium-doped fiber amplifiers: comparison of models and numerical simulation methods

S Balac

► **To cite this version:**

S Balac. Light-wave propagation in Erbium-doped fiber amplifiers: comparison of models and numerical simulation methods. IRMAR - Université Rennes 1. 2020. hal-04636447

HAL Id: hal-04636447

<https://hal.science/hal-04636447>

Submitted on 5 Jul 2024

HAL is a multi-disciplinary open access archive for the deposit and dissemination of scientific research documents, whether they are published or not. The documents may come from teaching and research institutions in France or abroad, or from public or private research centers.

L'archive ouverte pluridisciplinaire **HAL**, est destinée au dépôt et à la diffusion de documents scientifiques de niveau recherche, publiés ou non, émanant des établissements d'enseignement et de recherche français ou étrangers, des laboratoires publics ou privés.

Light-wave propagation in Erbium-doped fiber amplifiers : comparison of models and numerical simulation methods

S. Balac

October 12, 2020

Abstract

We compare different numerical approaches to solve two boundary value problems that modelize light-wave propagation in Erbium-doped fiber amplifiers. We consider two models, a basic model for Erbium-doped fiber amplifiers very widely used in the literature and a more advanced model that takes into account the amplified spontaneous emission (ASE) phenomenon.

Contents

1	Introduction	2
2	The basic model for Erbium-doped fiber amplifiers	2
2.1	Amplification model in three-level atomic systems	2
2.2	Reduction of the three-level system to the two level system	5
2.3	Analytical expression of the total output power	7
3	Numerical approaches for computing the pump and signal powers in the fiber	9
3.1	Co-propagative vs contra-propagative case : Cauchy problem vs boundary value problem	9
3.2	The (standard) Shooting method	10
3.3	A variant of the Shooting method	12
3.4	The Relaxation method	13
3.5	Numerical illustration	20
4	A model including amplified spontaneous emission	26
4.1	The model	26
4.2	Analytical expression of the total output power	28
4.3	General framework for numerical simulation	31
4.4	Simulation using a Shooting method	33
4.5	Simulation using a Relaxation method	33
4.6	Numerical experiments	38
	References	41

1 Introduction

Our concern in this document is the investigation of numerical methods for the simulation of light-wave propagation in Erbium-doped fiber amplifiers. From a mathematical point of view, light-wave propagation in Erbium-doped fiber amplifiers can be described through a system of non-linear ordinary equations (ode). The specificity of the situation is that this non-linear system of ode is not related to a Cauchy problem but to a boundary value problem: data are provided at both ends of the fiber. From a numerical point of view, the situation is therefore a little more difficult to handle than the situation of a Cauchy problem where standard methods such as the Runge-Kutta methods can be used straightaway. In order to solve this boundary value problem for a non-linear ode system, we investigate two groups of numerical methods: shooting methods on the one hand and relaxation methods on the other hand.

Roughly speaking, the principle of the shooting methods is as follows: (1) change the boundary value problem into a Cauchy problem by choosing some arbitrary values for the missing data at the fiber entry, (2) propagate the corresponding light-wave signal into the fiber, (3) compare the solution to the boundary value at the fiber end. The chosen values for the missing data at the fiber entry are then modified according to the gap between the computed values and the expected ones at the fiber end and the process is iterated until the gap is sufficiently small.

The principle of the relaxation methods is the following. A subdivision of the fiber length is introduced and a discretization scheme for ode (e.g. a Runge-Kutta scheme) is chosen and written down. Taking into account the boundary conditions, this leads to a non-linear system of equations that is solved using a standard numerical method such as Newton-Raphson method or the Secant method. Note that these numerical methods for solving non-linear systems of equations are iterative so that the two groups of methods are based on iterations.

The document is organized as follows. In Section 2, we introduce the mathematical model for light-wave propagation in Erbium-doped fiber amplifiers based on the book of Becker, Olsson and Simpson [1]. Description of the physical phenomena involved in Erbium-doped fiber amplifiers as well as notations are extracted from this reference [1]. In Section 3, we consider the simplified situation where the amplified spontaneous emission (ASE) phenomenon is neglected. We then have a system of only two ode (one for the pump and one for the signal) that allows us to introduce the above mentioned numerical methods in a simplified framework. After a description of the various methods that can be used to simulate light-wave propagation in Erbium-doped fiber amplifiers in this simplified situation, we compare their efficiency on a benchmark problem. In Section 4, we consider the more realistic situation where ASE is taken into account. After having highlighted the main difference with the simplified case from a numerical point of view, we provide simulation results obtained by the above mentioned numerical methods.

2 The basic model for Erbium-doped fiber amplifiers

2.1 Amplification model in three-level atomic systems

The energy levels of rare earth ions are composed of relatively well-separated multiplets, each of which is made up of a certain number of broadened individual levels. The most simple treatment of the erbium-doped fiber amplifier starts out by considering a pure three-level atomic system, see e.g. [1, Chapter 5] or [2, Chapter 1]. Most of the important characteristics of the amplifier can be obtained from this simple model and its underlying assumptions. This three-level system is intended to represent the part of the energy level structure of Er^{3+} that is relevant to the amplification process.

Thus, we consider a three-level system as depicted in Figure 1, with a ground state denoted by 1, an intermediate state labeled 3 (into which energy is pumped), and state 2. Since state 2 often has a long lifetime in the case of a good amplifier, it is sometimes referred to as the metastable level. State 2 is the upper level of the amplifying transition and state 1 is the lower

level. The populations density (number of ions per unit volume) of the three levels are labeled N_1 , N_2 , and N_3 respectively. To obtain amplification, we need a population inversion between states 1 and 2, and since state 1 is also the ground state, at least half of the total population of erbium ions needs to be excited to level 2 to have population inversion.

One can take particular advantage, in the case of the erbium-doped fiber amplifier, of the fact that the light fields are confined in a core of very small dimensions. The light intensities reached are thus very high, over long distances, and population inversion is achieved with relatively small pump powers. We will thus consider the problem to be one-dimensional. That is, we assume that the pump and signal intensities as well as the erbium ion distribution are constant in the transverse dimensions, over an effective cross-sectional area of the fiber.

We introduce the following quantities.

- The incident light intensity flux at the frequency corresponding to the 1 to 3 transition (in number of photons per unit time per unit area) is denoted by ϕ_p and corresponds to the pump.
- The incident flux at the frequency corresponding to the 1 to 2 transition (in photons per unit time per unit area) is denoted by ϕ_s and corresponds to the signal field.

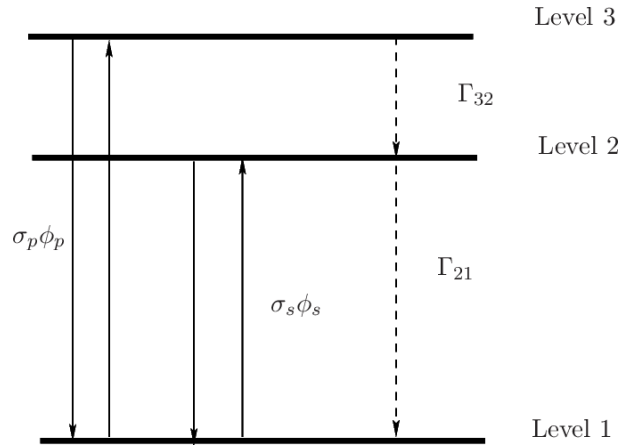


Figure 1: The three levels system used for the amplifier model.

The change in population for each level arises from absorption of photons from the incident light field, from spontaneous and stimulated emission, and from other pathways for the energy to escape a particular level. In particular, we denote by

- Γ_{32} the transition probability from level 3 to level 2;
- Γ_{21} the transition probability from level 2 to level 1;
- $\tau_2 = \frac{1}{\Gamma_{21}}$ the lifetime of level 2.

We also denote

- σ_p the absorption cross section for the 1 to 3 transition
- σ_s the emission cross section for the 2 to 1 transition

In this basic model, we assume that the transition rates between levels 1 and 3 are proportional to the populations in those levels and to the product of the pump flux ϕ_p by the pump cross section σ_p . The transition rates between levels 1 and 2 are proportional to the populations in those levels and to the product of the signal flux ϕ_s by the signal cross section σ_s . The

spontaneous transition rates of the ion (including radiative and nonradiative contributions) are given by Γ_{32} and Γ_{21} . Moreover, we assume that the absorption and emission cross sections we consider are those for transitions between individual non-degenerate states and are thus equal.¹ These considerations lead to the following system of equations for the population changes in the three levels:²

$$\left\{ \begin{array}{l} \frac{\partial N_3}{\partial t}(z, t) = -\Gamma_{32} N_3(z, t) + (N_1(z, t) - N_3(z, t))\sigma_p \phi_p(z, t) \\ \frac{\partial N_2}{\partial t}(z, t) = -\Gamma_{21} N_2(z, t) + \Gamma_{32} N_3(z, t) + (N_2(z, t) - N_1(z, t))\sigma_s \phi_s(z, t) \\ \frac{\partial N_1}{\partial t}(z, t) = -\Gamma_{21} N_2(z, t) + (N_1(z, t) - N_3(z, t))\sigma_p \phi_p(z, t) \\ \quad \quad \quad + (N_2(z, t) - N_1(z, t))\sigma_s \phi_s(z, t) \end{array} \right. \quad \begin{array}{l} (1a) \\ (1b) \\ (1c) \end{array}$$

for all $z \in [0, L]$ where L is the length of the fiber and for all time $t \geq 0$. These equations are referred to as the *rate equations*.

We are interested in the steady-state situation. The population N is then given by

$$N = N_1(t) + N_2(t) + N_3(t) \quad \forall t \in \mathbb{R}^+. \quad (2)$$

Equations (1) can be solved analytically in the steady-state regime. In particular, we deduce from equation (1a) that

$$N_3(z) = \frac{1}{1 + \frac{\Gamma_{32}}{\sigma_p \phi_p(z)}} \quad (3)$$

When Γ_{32} is large (reflecting a fast decay from level 3 to level 2) compared to the effective pump rate into level 3 (defined as $\sigma_p \phi_p(z)$), the population density N_3 is very close to zero, so that the population is mostly in levels 1 and 2. This situation which is really likely to occur in practice allows a reduction of the three-level system to the two level system, see Section 2.2.

We also need the propagation equations for the two light fields (the pump and the signal field) propagating through the fiber and interacting with the ions. The light fields corresponding to the signal field and to the pump field will be attenuated or amplified after an infinitesimal length dz by the combined effects of absorption arising from ions in their ground state N_1 and stimulated emission from ions in the excited state (N_2 and N_3). This leads, to the following propagation equations:

$$\left\{ \begin{array}{l} \frac{\partial \phi_s}{\partial z}(z, t) = (N_2(z, t) - N_1(z, t))\sigma_s \phi_s(z, t) \\ \frac{\partial \phi_p}{\partial z}(z, t) = (N_3(z, t) - N_1(z, t))\sigma_p \phi_p(z, t) \end{array} \right. \quad \begin{array}{l} (4a) \\ (4b) \end{array}$$

when both pump and signal beams are propagating in the same direction, i.e., a co-propagating configuration as opposed to a counter-propagating configuration. In the counter-propagating configuration, the propagation equations read

$$\left\{ \begin{array}{l} \frac{\partial \phi_s}{\partial z}(z, t) = (N_2(z, t) - N_1(z, t))\sigma_s \phi_s(z, t) \\ \frac{\partial \phi_p}{\partial z}(z, t) = -(N_3(z, t) - N_1(z, t))\sigma_p \phi_p(z, t) \end{array} \right. \quad \begin{array}{l} (5a) \\ (5b) \end{array}$$

¹We will consider latter the more practical case of erbium levels that consist of a set of states where the absorption and emission cross sections are different, as they incorporate information on the thermal population distribution.

²The rate equations can also be made more complex by considering such effects as excited state absorption and the three-dimensional character of the problem. These effects will be discussed latter. The possible stimulated emission at the pump wavelength will also be treated latter.

Note that these two configurations can be handled in a unique way by introducing a factor u with values $u = +1$ in the co-propagating case and $u = -1$ in the contra-propagating case. The propagation equation for the pump field then reads

$$\frac{\partial \phi_p}{\partial z}(z, t) = u (N_3(z, t) - N_1(z, t)) \sigma_p \phi_p(z, t) \quad (6)$$

in the two cases.

2.2 Reduction of the three-level system to the two level system

When we assume that the pumping level 3 belongs to a multiplet different than that of level 2, and that there is rapid relaxation from level 3 to level 2, for all practical purposes, the population in level 3 can be assumed to be zero and the rate equations (1) involve only the two levels 1 and 2, with level 3 being involved only via the value of the pump absorption cross section from level 1 to level 3.

On the contrary, in certain pumping configurations, level 3 can be identical to level 2 in the sense that the upper pump level and the upper amplifier level belong to the same multiplet. In this case, the population of level 3 will not necessarily be equal to zero but assuming that the thermal equilibrium time established within a given multiplet is very short compared to the overall multiplet, the pumping will have some finite thermal population. There will then be stimulated emission at the pump frequency as well as at the signal frequency, the amount of which depends on the thermal population of the various states involved as well as the strength of their interaction with a light field. The behavior of the entire system can be represented through the absorption and emission cross sections (these two quantities contain the thermal population distribution information). To this end, we denote by $\sigma_s^{(a)}$, $\sigma_s^{(e)}$, $\sigma_p^{(a)}$ and $\sigma_p^{(e)}$ respectively the signal and pump absorption and emission cross sections parameters. In general, the emission and absorption cross sections parameters will be related by the McCumber relationship.

Based on these two practical situations, we will refer only to the total populations of levels 1 and 2, and use the cross sections parameters to model the system's interaction with the pump and signal fields. The rate equations for the two level system corresponding to the reduction of the three-level system (1) with the introduction of the emission and absorption cross sections parameters reads

$$\left\{ \begin{array}{l} \frac{\partial N_2}{\partial t}(z, t) = -\Gamma_{21} N_2(z, t) + (\sigma_s^{(a)} N_1(z, t) - \sigma_s^{(e)} N_2(z, t)) \phi_s(z, t) \\ \quad - (\sigma_p^{(e)} N_2(z, t) - \sigma_p^{(a)} N_1(z, t)) \phi_p(z, t) \\ \frac{\partial N_1}{\partial t}(z, t) = \Gamma_{21} N_2(z, t) + (\sigma_s^{(e)} N_2(z, t) - \sigma_s^{(a)} N_1(z, t)) \phi_s(z, t) \\ \quad - (\sigma_p^{(a)} N_1(z, t) - \sigma_p^{(e)} N_2(z, t)) \phi_p(z, t) \end{array} \right. \quad (7a)$$

$$\left\{ \begin{array}{l} \frac{\partial N_2}{\partial t}(z, t) = -\Gamma_{21} N_2(z, t) + (\sigma_s^{(a)} N_1(z, t) - \sigma_s^{(e)} N_2(z, t)) \phi_s(z, t) \\ \quad - (\sigma_p^{(e)} N_2(z, t) - \sigma_p^{(a)} N_1(z, t)) \phi_p(z, t) \\ \frac{\partial N_1}{\partial t}(z, t) = \Gamma_{21} N_2(z, t) + (\sigma_s^{(e)} N_2(z, t) - \sigma_s^{(a)} N_1(z, t)) \phi_s(z, t) \\ \quad - (\sigma_p^{(a)} N_1(z, t) - \sigma_p^{(e)} N_2(z, t)) \phi_p(z, t) \end{array} \right. \quad (7b)$$

Note that the case where level 3 belongs to a higher-lying multiplet can be reduced to the two-level picture just described by simply setting the pump emission cross section to zero, which effectively accounts for the fact that the population of level 3 is in this case equal to zero.

The propagation equations (5) for the pump and signal are modified accordingly to distinguish between the absorption and emission cross sections in the general situation where $\sigma_s^{(a)} \neq \sigma_s^{(e)}$ and $\sigma_p^{(a)} \neq \sigma_p^{(e)}$. Moreover, it is important to realize that even in a simple one-dimensional model of the fiber amplifier, the transverse shape of the optical mode and its overlap with the transverse erbium ion distribution profile are important and must be taken into account in the model. In general, this phenomenon can be taken into account simply by introducing a factor known as the *overlap factor* [3]. Only the portion given by the overlap factor of the optical mode that overlaps with the erbium ion distribution will stimulate absorption or emission from

the Er^{3+} transitions. We denote by Γ_s the overlap factor representing the overlap between the erbium ions and the mode of the source field and we denote by Γ_p the overlap factor representing the overlap between the erbium ions and the mode of the pump field. Taking into consideration these two new aspects in the model, the propagation equations (5) are finally upgraded in the following propagation equations:

$$\left\{ \begin{array}{l} \frac{\partial \phi_s}{\partial z}(z, t) = (\sigma_s^{(e)} N_2(z, t) - \sigma_s^{(a)} N_1(z, t)) \Gamma_s \phi_s(z, t) \\ \frac{\partial \phi_p}{\partial z}(z, t) = u (\sigma_p^{(e)} N_2(z, t) - \sigma_p^{(a)} N_1(z, t)) \Gamma_p \phi_p(z, t) \end{array} \right. \quad (8a)$$

$$\left\{ \begin{array}{l} \frac{\partial \phi_s}{\partial z}(z, t) = (\sigma_s^{(e)} N_2(z, t) - \sigma_s^{(a)} N_1(z, t)) \Gamma_s \phi_s(z, t) \\ \frac{\partial \phi_p}{\partial z}(z, t) = u (\sigma_p^{(e)} N_2(z, t) - \sigma_p^{(a)} N_1(z, t)) \Gamma_p \phi_p(z, t) \end{array} \right. \quad (8b)$$

The incident signal light intensity flux ϕ_s is given by

$$\phi_s = \frac{I_s}{h\nu_s} \quad (9a)$$

where I_s is the signal field intensity and ν_s the signal field frequency. In the one-dimensional case, the signal field intensity is deduced from the signal field power by the following simplified relationship:

$$I_s = \frac{\Gamma_s}{A_{\text{eff}}} P_s \quad (9b)$$

where A_{eff} is the effective cross-sectional area of the distribution of erbium ions. Similarly, the incident pump light intensity flux ϕ_p is given by

$$\phi_p = \frac{I_p}{h\nu_p} \quad (9c)$$

where I_p is the pump field intensity and ν_p the pump field frequency, and the pump field intensity is deduced from the pump field power by the following simplified relationship:

$$I_p = \frac{\Gamma_p}{A_{\text{eff}}} P_p. \quad (9d)$$

The propagation equations for the pump and signal powers deduced from (8) then read

$$\left\{ \begin{array}{l} \frac{\partial P_s}{\partial z}(z, t) = ((\sigma_s^{(e)} + \sigma_s^{(a)}) N_2(z, t) - \sigma_s^{(a)} N) \Gamma_s P_s(z, t) \\ \frac{\partial P_p}{\partial z}(z, t) = u ((\sigma_p^{(e)} + \sigma_p^{(a)}) N_2(z, t) - \sigma_p^{(a)} N) \Gamma_p P_p(z, t) \end{array} \right. \quad (10a)$$

$$\left\{ \begin{array}{l} \frac{\partial P_s}{\partial z}(z, t) = ((\sigma_s^{(e)} + \sigma_s^{(a)}) N_2(z, t) - \sigma_s^{(a)} N) \Gamma_s P_s(z, t) \\ \frac{\partial P_p}{\partial z}(z, t) = u ((\sigma_p^{(e)} + \sigma_p^{(a)}) N_2(z, t) - \sigma_p^{(a)} N) \Gamma_p P_p(z, t) \end{array} \right. \quad (10b)$$

where $N = N_1(z, t) + N_2(z, t)$ is the total ion population density assumed to be independent of the position z along the fiber.

If we introduce the proportion \bar{N}_2 of ions in Level 2 defined as $\bar{N}_2 = N_2/N$, then the propagation equations for the pump and signal powers read

$$\left\{ \begin{array}{l} \frac{\partial P_s}{\partial z}(z, t) = N ((\sigma_s^{(e)} + \sigma_s^{(a)}) \bar{N}_2(z, t) - \sigma_s^{(a)}) \Gamma_s P_s(z, t) \\ \frac{\partial P_p}{\partial z}(z, t) = u N ((\sigma_p^{(e)} + \sigma_p^{(a)}) \bar{N}_2(z, t) - \sigma_p^{(a)}) \Gamma_p P_p(z, t) \end{array} \right. \quad (11a)$$

$$\left\{ \begin{array}{l} \frac{\partial P_s}{\partial z}(z, t) = N ((\sigma_s^{(e)} + \sigma_s^{(a)}) \bar{N}_2(z, t) - \sigma_s^{(a)}) \Gamma_s P_s(z, t) \\ \frac{\partial P_p}{\partial z}(z, t) = u N ((\sigma_p^{(e)} + \sigma_p^{(a)}) \bar{N}_2(z, t) - \sigma_p^{(a)}) \Gamma_p P_p(z, t) \end{array} \right. \quad (11b)$$

These equations coincide with equations (5.59) – (5.60) in [1] up to the change in the notations ($N_2 \rightarrow \bar{N}_2$, $\rho \rightarrow N$).

In the steady-state regime, the rate equations (7) can be solved analytically. We have $N = N_1(z, t) + N_2(z, t)$ for all $t \in \mathbb{R}^+$ and we deduce from (7a) that

$$N_2(z, t) = \frac{\sigma_s^{(a)} \phi_s(z, t) + \sigma_p^{(a)} \phi_p(z, t)}{\Gamma_{21} + (\sigma_s^{(a)} + \sigma_s^{(e)}) \phi_s(z, t) + (\sigma_p^{(a)} + \sigma_p^{(e)}) \phi_p(z, t)} N \quad (12a)$$

$$= \frac{\sigma_s^{(a)} \frac{\Gamma_s}{h\nu_s} P_s(z, t) + \sigma_p^{(a)} \frac{\Gamma_p}{h\nu_p} P_p(z, t)}{A_{\text{eff}} \Gamma_{21} + (\sigma_s^{(a)} + \sigma_s^{(e)}) \frac{\Gamma_s}{h\nu_s} P_s(z, t) + (\sigma_p^{(a)} + \sigma_p^{(e)}) \frac{\Gamma_p}{h\nu_p} P_p(z, t)} N \quad (12b)$$

These relations coincide respectively with (5.52) and (6.3) in [1].

We define the pump attenuation constant $\alpha_p^{(a)}$ and the signal attenuation constant $\alpha_s^{(a)}$ for the pump and signal (in unit m^{-1}) as

$$\alpha_p^{(a)} = N \Gamma_p \sigma_p^{(a)} \quad (13a)$$

$$\alpha_s^{(a)} = N \Gamma_s \sigma_s^{(a)} \quad (13b)$$

and the saturation powers for the pump and signal (in unit W) as

$$P_p^{\text{sat}} = \frac{A_{\text{eff}} \Gamma_{21} h\nu_p}{(\sigma_p^{(a)} + \sigma_p^{(e)}) \Gamma_p} \quad (14a)$$

$$P_s^{\text{sat}} = \frac{A_{\text{eff}} \Gamma_{21} h\nu_s}{(\sigma_s^{(a)} + \sigma_s^{(e)}) \Gamma_s} \quad (14b)$$

Then, the ion population at level 2 given by (12b) can be expressed (in unit m^{-3}) as

$$N_2(z, t) = \frac{\tau_2}{A_{\text{eff}}} \frac{\frac{\alpha_p^{(a)}}{h\nu_p} P_p(z, t) + \frac{\alpha_s^{(a)}}{h\nu_s} P_s(z, t)}{1 + \frac{P_s(z, t)}{P_s^{\text{sat}}} + \frac{P_p(z, t)}{P_p^{\text{sat}}}} \quad (15)$$

where A_{eff} is the cross-sectional area of the erbium ion distribution in the fiber and $\tau_2 = \frac{1}{\Gamma_{21}}$ is the lifetime of level 2.

We can then substitute N_2 as given by (15) in the propagation equations (10) to obtain the following non-linear system of ODE

$$\left\{ \begin{array}{l} \frac{\partial P_s}{\partial z}(z, t) = -\alpha_s^{(a)} P_s(z, t) + \frac{\alpha_s^{(a)} P_s(z, t) + \frac{\nu_s}{\nu_p} \alpha_p^{(a)} P_p(z, t)}{1 + \frac{P_s(z, t)}{P_s^{\text{sat}}} + \frac{P_p(z, t)}{P_p^{\text{sat}}}} \frac{P_s(z, t)}{P_s^{\text{sat}}} \\ u \frac{\partial P_p}{\partial z}(z, t) = -\alpha_p^{(a)} P_p(z, t) + \frac{\alpha_p^{(a)} P_p(z, t) + \frac{\nu_p}{\nu_s} \alpha_s^{(a)} P_s(z, t)}{1 + \frac{P_s(z, t)}{P_s^{\text{sat}}} + \frac{P_p(z, t)}{P_p^{\text{sat}}}} \frac{P_p(z, t)}{P_p^{\text{sat}}} \end{array} \right. \quad (16a)$$

$$\left. \begin{array}{l} \frac{\partial P_s}{\partial z}(z, t) = -\alpha_s^{(a)} P_s(z, t) + \frac{\alpha_s^{(a)} P_s(z, t) + \frac{\nu_s}{\nu_p} \alpha_p^{(a)} P_p(z, t)}{1 + \frac{P_s(z, t)}{P_s^{\text{sat}}} + \frac{P_p(z, t)}{P_p^{\text{sat}}}} \frac{P_s(z, t)}{P_s^{\text{sat}}} \\ u \frac{\partial P_p}{\partial z}(z, t) = -\alpha_p^{(a)} P_p(z, t) + \frac{\alpha_p^{(a)} P_p(z, t) + \frac{\nu_p}{\nu_s} \alpha_s^{(a)} P_s(z, t)}{1 + \frac{P_s(z, t)}{P_s^{\text{sat}}} + \frac{P_p(z, t)}{P_p^{\text{sat}}}} \frac{P_p(z, t)}{P_p^{\text{sat}}} \end{array} \right. \quad (16b)$$

2.3 Analytical expression of the total output power

Let us consider back equation (7a). Combining it with (8), we obtain

$$\frac{\partial N_2}{\partial t}(z, t) = -\Gamma_{21} N_2(z, t) - \frac{1}{\Gamma_s} \frac{\partial \phi_s}{\partial z}(z, t) - \frac{u}{\Gamma_p} \frac{\partial \phi_p}{\partial z}(z, t). \quad (17)$$

From relations (9), we have

$$\phi_s(z, t) = \frac{\Gamma_s}{h\nu_s A_{\text{eff}}} P_s(z, t) \quad \text{and} \quad \phi_p(z, t) = \frac{\Gamma_p}{h\nu_p A_{\text{eff}}} P_p(z, t) \quad (18)$$

so that

$$\frac{\partial N_2}{\partial t}(z, t) = -\frac{1}{\tau_2} N_2(z, t) - \frac{1}{A_{\text{eff}}} \left(\frac{1}{h\nu_s} \frac{\partial P_s}{\partial z}(z, t) + \frac{u}{h\nu_p} \frac{\partial P_p}{\partial z}(z, t) \right) \quad (19)$$

where $\tau_2 = \frac{1}{\Gamma_{21}}$ is the lifetime of level 2.

This equation slightly differs from (5.61) in [1]. The coefficients highlighted in red are not given in [1].

In the steady state regime, we deduce that

$$N_2(z, t) = -\frac{\tau_2}{A_{\text{eff}}} \left(\frac{1}{h\nu_s} \frac{\partial P_s}{\partial z}(z, t) + \frac{u}{h\nu_p} \frac{\partial P_p}{\partial z}(z, t) \right) \quad (20)$$

Let us now consider once again the propagation equations for the pump and signal powers as given by (10). Substituting the expression of N_2 as given by (20), we obtain

$$\left\{ \begin{array}{l} \frac{\partial P_s}{\partial z}(z, t) = - \left(\alpha_s^{(a)} + \frac{1}{P_s^{\text{sat}}} \left(\frac{\partial P_s}{\partial z}(z, t) + u \frac{\nu_s}{\nu_p} \frac{\partial P_p}{\partial z}(z, t) \right) \right) P_s(z, t) \\ u \frac{\partial P_p}{\partial z}(z, t) = - \left(\alpha_p^{(a)} + \frac{1}{P_p^{\text{sat}}} \left(\frac{\nu_p}{\nu_s} \frac{\partial P_s}{\partial z}(z, t) + u \frac{\partial P_p}{\partial z}(z, t) \right) \right) P_p(z, t) \end{array} \right. \quad (21a)$$

$$\left. \right\} \quad (21b)$$

Let us denote by P_s^{in} and P_s^{out} the input and output powers of the signal field at the fiber ends $z = 0$ and $z = L$ respectively; Namely $P_s(z = 0, t) = P_s^{\text{in}}(t)$ and $P_s(z = L, t) = P_s^{\text{out}}(t)$ for all time $t \geq 0$. Similarly, we denote by P_p^{in} and P_p^{out} the input and output powers of the signal field at the fiber ends. If the pump field is co-propagating ($u = +1$), we have $P_p(z = 0, t) = P_p^{\text{in}}(t)$ and $P_p(z = L, t) = P_p^{\text{out}}(t)$ for all time $t \geq 0$ whereas if the pump field is contra-propagating ($u = -1$), we have $P_p(z = L, t) = P_p^{\text{in}}(t)$ and $P_p(z = 0, t) = P_p^{\text{out}}(t)$ for all time $t \geq 0$.

Let us now divide (21a) by P_s and integrate both side of the equation from $z = 0$ to $z = L$. We obtain in the two cases $u = \pm 1$

$$\ln \left(\frac{P_s^{\text{out}}(t)}{P_s^{\text{in}}(t)} \right) = -\alpha_s^{(a)} L - \frac{1}{P_s^{\text{sat}}} \left(P_s^{\text{out}}(t) - P_s^{\text{in}}(t) + \frac{\nu_s}{\nu_p} (P_p^{\text{out}}(t) - P_p^{\text{in}}(t)) \right) \quad (22)$$

Thus,

$$P_s^{\text{out}}(t) = P_s^{\text{in}}(t) e^{-\alpha_s^{(a)} L} e^{-\frac{\nu_s^{-1}(P_s^{\text{out}}(t) - P_s^{\text{in}}(t)) + \nu_p^{-1}(P_p^{\text{out}}(t) - P_p^{\text{in}}(t))}{\nu_s^{-1} P_s^{\text{sat}}}} \quad (23)$$

$$= P_s^{\text{in}}(t) e^{-\alpha_s^{(a)} L} e^{-\frac{E^{\text{out}}(t) - E^{\text{in}}(t)}{E_s^{\text{sat}}}} \quad (24)$$

where

$$\begin{aligned} E^{\text{out}} &= \nu_s^{-1} P_s^{\text{out}} + \nu_p^{-1} P_p^{\text{out}} \\ E^{\text{in}} &= \nu_s^{-1} P_s^{\text{in}} + \nu_p^{-1} P_p^{\text{in}} \\ E_s^{\text{sat}} &= \nu_s^{-1} P_s^{\text{sat}} \end{aligned}$$

Note that the quantities E^{out} , E^{in} and E_s^{sat} are equivalent to energies (in unit J). Similarly, we obtain

$$P_p^{\text{out}}(t) = P_p^{\text{in}}(t) e^{-\alpha_p^{(a)} L} e^{-\frac{E^{\text{out}}(t) - E^{\text{in}}(t)}{E_p^{\text{sat}}}} \quad (25)$$

where

$$E_p^{\text{sat}} = \nu_p^{-1} P_p^{\text{sat}} \quad (26)$$

By summing (23) multiplied by ν_s^{-1} and (25) multiplied by ν_p^{-1} , we obtain

$$E^{\text{out}}(t) = \nu_s^{-1} P_s^{\text{in}}(t) e^{-\alpha_s^{(a)} L} e^{-\frac{E^{\text{out}}(t) - E^{\text{in}}(t)}{E_s^{\text{sat}}}} + \nu_p^{-1} P_p^{\text{in}}(t) e^{-\alpha_p^{(a)} L} e^{-\frac{E^{\text{out}}(t) - E^{\text{in}}(t)}{E_p^{\text{sat}}}} \quad (27)$$

We can solve (numerically) this non-linear equation to obtain the (exact) values of E_*^{out} for all $t \in \mathbb{R}^+$. This provides a reference case to test the accuracy of a purely numerical approach to solve the non-linear system of ODE (16).

Note that for numerical computation purposes, it is more convenient to express the non linear equation (27) in a slightly different way. Multiplying both side by ν_p , we obtain

$$\tilde{P}^{\text{out}}(t) = \frac{\nu_p}{\nu_s} P_s^{\text{in}}(t) e^{-\alpha_s^{(a)} L} e^{-\frac{\nu_s}{\nu_p} \frac{\tilde{P}^{\text{out}}(t) - \tilde{P}^{\text{in}}(t)}{P_s^{\text{sat}}}} + P_p^{\text{in}}(t) e^{-\alpha_p^{(a)} L} e^{-\frac{\tilde{P}^{\text{out}}(t) - \tilde{P}^{\text{in}}(t)}{P_p^{\text{sat}}}} \quad (28)$$

where

$$\begin{aligned} \tilde{P}^{\text{out}} &= \nu_p E^{\text{out}} = \frac{\nu_p}{\nu_s} P_s^{\text{out}} + P_p^{\text{out}} \\ \tilde{P}^{\text{in}} &= \nu_p E^{\text{in}} = \frac{\nu_p}{\nu_s} P_s^{\text{in}} + P_p^{\text{in}} \end{aligned}$$

3 Numerical approaches for computing the pump and signal powers in the fiber

3.1 Co-propagative vs contra-propagative case : Cauchy problem vs boundary value problem

Computation of the pump and signal powers along the fiber, i.e. computation of $P_s(z, t)$ and $P_p(z, t)$ for all $z \in [0, L]$, requires the solving of the non-linear system of ODE (16). Closed-form solution to this non-linear system of ODE can not be obtained and a numerical approach is mandatory. This autonomous non-linear system of ODE can be expressed as

$$Y_t'(z) = -A Y_t(z) + F(Y_t(z)) \quad (29)$$

where for any fixed $t \in \mathbb{R}^+$ the unknown function Y_t is defined as

$$Y_t : z \in [0, L] \mapsto \begin{pmatrix} P_s(z, t) \\ P_p(z, t) \end{pmatrix}, \quad (30)$$

A denotes the 2×2 diagonal matrix with diagonal entries $\alpha_s^{(a)}$ and $u \alpha_p^{(a)}$ and F is the mapping

$$F : X = (x_1, x_2) \in \mathbb{R}^2 \mapsto \begin{pmatrix} \frac{1}{P_s^{\text{sat}}} \frac{\alpha_s^{(a)} x_1^2 + \frac{\nu_s}{\nu_p} \alpha_p^{(a)} x_1 x_2}{1 + \frac{1}{P_s^{\text{sat}}} x_1 + \frac{1}{P_p^{\text{sat}}} x_2} \\ u \frac{1}{P_p^{\text{sat}}} \frac{\alpha_p^{(a)} x_2^2 + \frac{\nu_s}{\nu_p} \alpha_s^{(a)} x_1 x_2}{1 + \frac{1}{P_s^{\text{sat}}} x_1 + \frac{1}{P_p^{\text{sat}}} x_2} \end{pmatrix} \in \mathbb{R}^2. \quad (31)$$

We now have to distinguish the two cases of co-propagating fields ($u = +1$) and contra-propagating fields ($u = -1$). In the co-propagating case, the boundary conditions are

$$P_s(z = 0, t) = P_s^{\text{in}}(t) \quad \text{and} \quad P_p(z = 0, t) = P_p^{\text{in}}(t) \quad \forall t \in \mathbb{R}^+ \quad (32)$$

where P_s^{in} and P_p^{in} are the incoming given signal and pump powers at the fiber entry located at $z = 0$. Thus, the non-linear ODE system (29) with boundary conditions (107) form a Cauchy problem that can be solved numerically using classical schemes for ODE such as Runge-Kutta schemes. We will not treat this case here since it is very conventional and there's nothing special to say about it.

In the contra-propagating case, the boundary conditions are

$$P_s(z = 0, t) = P_s^{\text{in}}(t) \quad \text{and} \quad P_p(z = L, t) = P_p^{\text{in}}(t) \quad \forall t \in \mathbb{R}^+. \quad (33)$$

We have one condition at each fiber ends and the problem is not anymore a Cauchy problem but a boundary value problem. A simple numerical approach for solving such a problem is referred to as the *Shooting method*. It is detailed in Section 3.2 below. Another classical numerical approach is the so-called *relaxation method*. It is actually a family of numerical methods that will be introduced in Section 3.4.

3.2 The (standard) Shooting method

Let us briefly introduce the Shooting method for solving our problem in the contra-propagating case. With the notation introduced earlier, our problem reads : Find a differentiable mapping $Y : z \in [0, L] \rightarrow Y(z) = \begin{pmatrix} y_1(z) \\ y_2(z) \end{pmatrix} \in \mathbb{R}^2$ such that

$$\begin{cases} Y'(z) = -A Y(z) + F(Y(z)) & \forall z \in]0, L[& (34a) \\ y_1(z = 0) = P_s^{\text{in}} & & (34b) \\ y_2(z = L) = P_p^{\text{in}} & & (34c) \end{cases}$$

where P_s^{in} and P_p^{in} are known data. We consider the following family of Cauchy problems parameterized by $\lambda \in \mathbb{R}$: Find a differentiable mapping

$$U_\lambda : z \in [0, L] \rightarrow U_\lambda(z) = \begin{pmatrix} u_{\lambda,1}(z) \\ u_{\lambda,2}(z) \end{pmatrix} \in \mathbb{R}^2$$

such that

$$(\mathcal{Q}_\lambda) \begin{cases} U'_\lambda(z) = -A U_\lambda(z) + F(U_\lambda(z)) & \forall z \in]0, L[& (35a) \\ u_{\lambda,1}(z = 0) = P_s^{\text{in}} & & (35b) \\ u_{\lambda,2}(z = 0) = \lambda & & (35c) \end{cases}$$

One can easily see that U_λ solution to Cauchy problem (\mathcal{Q}_λ) is a solution to problem (34) if and only if $u_{\lambda,2}(z = L) = P_p^{\text{in}}$. Therefore, we are looking for $\lambda \in \mathbb{R}$ such that

$$u_{\lambda,2}(z = L) - P_p^{\text{in}} = 0 \quad (36)$$

that is to say, the roots of the mapping $f : \lambda \in \mathbb{R} \mapsto u_{\lambda,2}(z = L) - P_p^{\text{in}}$. Equation (36) is a non-linear equation that can be solved numerically to determine its roots λ . Among the classical methods for solving non-linear equations is the Newton-Raphson method. A sequence $(\lambda_n)_{n \in \mathbb{N}}$ such that

$$\lambda_{n+1} = \lambda_n - \frac{f(\lambda_n)}{f'(\lambda_n)} \quad (37)$$

is iteratively computed from an initial value λ_0 and this sequence is likely to converge to a root λ of the mapping f when convergence conditions are satisfied. A drawback of Newton-Raphson method is that it requires the knowledge of the derivative f' , which is just about impossible here to compute. An alternative method is the Secant method where the derivative of f is replaced by an approximation computed from a finite difference formula. In the Secant method, a sequence $(\lambda_n)_{n \in \mathbb{N}}$ is computed according to the relation

$$\lambda_{n+1} = \lambda_n - f(\lambda_n) \frac{\lambda_n - \lambda_{n-1}}{f(\lambda_n) - f(\lambda_{n-1})}. \quad (38)$$

Hera again, the sequence is likely to converge to a root λ of the mapping f when convergence conditions are fulfilled. The convergence rate of the Secant method is smaller than the one of the Newton method, that is to say that the sequence $(\lambda_n)_{n \in \mathbb{N}}$ less quickly approaches the sought out root λ , but it has the advantage of not necessitating other information than the function itself.

The algorithm of the Shooting method combined with the Secant method for solving the boundary problem (34) may be described as follows.

- Initialization stage:
 - Chose a first arbitrary value λ_1 and solve Cauchy problem $(\mathcal{Q}_{\lambda_1})$ by any suitable method (e.g. a Runge-Kutta method).
 - Let v_1 denotes the approximation of $u_{\lambda_1,2}(z = L)$ obtained.
 - Chose a second arbitrary value λ_2 and solve Cauchy problem $(\mathcal{Q}_{\lambda_2})$.
 - Let v_2 denotes the approximation of $u_{\lambda_2,2}(z = L)$ obtained this way.
- Let $k = 3$ and $\lambda_k = \lambda_2 - (v_2 - P_p^{\text{in}}) \frac{\lambda_2 - \lambda_1}{v_2 - v_1}$.
- While a stopping criterium is not fulfilled do:
 - Solve Cauchy problem $(\mathcal{Q}_{\lambda_k})$.
 - $v_k = u_{\lambda_k,2}(z = L)$.
 - $k \leftarrow k + 1$
 - $\lambda_k = \lambda_{k-1} - (v_{k-1} - P_p^{\text{in}}) \frac{\lambda_{k-1} - \lambda_{k-2}}{v_{k-1} - v_{k-2}}$.

end do

Typically, iterations are stopped when two successive values v_k and v_{k-1} are considered not to differ sufficiently so that continuing the iterations provides a gain in accuracy. A tolerance value is set, e.g. $\text{tol} = 10^{-10}$, and when $|v_k - v_{k-1}| < \text{tol}$ iterations are stopped.

Note that each evaluation of the non-linear function $f(\lambda) = u_{\lambda,2}(z = L) - P_p^{\text{in}}$ requires to solve the Cauchy problem (\mathcal{Q}_λ) for that value of the parameter λ in order to get the value of $u_{\lambda,2}(z = L)$. This can be achieved by using a Runge-Kutta method as in the co-propagative case. The contra-propagative case is therefore likely to be much more expansive in computation than the co-propagative case. Fortunately, in the numerical experiments we have conducted, only a small number iterations (lower than 10) of the Secant method were necessary to compute an accurate solution in the contra-propagative case.

The Shooting method can be interpreted as follows. Since the value $y_2(z = 0)$ is unknown, a first guess λ_1 is chosen and the Cauchy problem deduced from the boundary problem (34) with this guess is solved, *i.e.* the initial data $(P_s^{\text{in}}, \lambda_1)$ is propagated or shoot. Of course, It is quite unlikely that this solution matches the boundary condition $y_2(z = L) = P_p^{\text{in}}$. The difference $f(\lambda_1) = y_2(z = L) - P_p^{\text{in}}$ is the algebraic distance to the target. A second shoot with a value λ_2 is achieved following the same principle. From these two initial shoots, we can deduce a third value λ_3 from the recurrence relation (38) and then iteratively compute λ_4 , etc. When the convergence conditions for the Secant method are fulfilled, each new shoot is closer and closer to the target. Finally, the computed solution almost matches the target condition $y_2(z = L) = P_p^{\text{in}}$. The stopping criteria can be interpreted as follows: when two successive shots come to almost the same position (almost being quantified by the tolerance value), there is no need to continue the shots since there is no significant improvement toward the target. The principle of the Shooting method is illustrated in Fig. 2.

Numerical examples illustrating the use of the Shooting method are provided in Section 3.5.

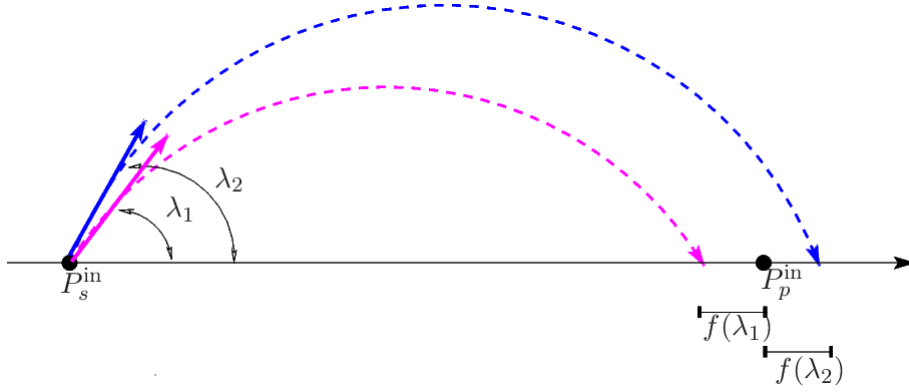


Figure 2: Illustration of the principle of the Shooting method. The first two shots are illustrated. The next shots are done with a parameter λ defined by the recurrence relation (38).

3.3 A variant of the Shooting method

In [2], a method for solving the boundary problem (34) is outlined. This method is incorrectly referred to as a Relaxation method. It is actually a variant of the Shooting method that avoid the need to solve a non-linear equation by the Secant method as it is the case for the standard Shooting method described in Section 3.2. The counterpart is an increasing number of iterations of the method. Note that Relaxation methods for solving the boundary problem (34) will be detailed in Section 3.4.

This Shooting method variant can be described as follows. We chose an arbitrary value for the parameter λ in the Cauchy problem (35) related to our boundary problem (34). We solve Cauchy problem (35) for that value of λ by a numerical method such as the RK4 method. This is the first shot. The value of the solution $U_\lambda^{(1)}(L) = \begin{pmatrix} u_{\lambda,1}^{(1)}(L) \\ u_{\lambda,2}^{(1)}(L) \end{pmatrix}$ at the fiber end is considered.

Here the exponent ⁽¹⁾ means that the results is related to the first shot attempt. We can expect that $u_{\lambda,2}^{(1)}(L) = P_p^{\text{in}}$ but there will be limited chances to happen. Therefore, we change $U_\lambda^{(1)}(L)$ for $U_\lambda^{(2)}(L) = \begin{pmatrix} u_{\lambda,1}^{(1)}(L) \\ P_p^{\text{in}} \end{pmatrix}$ and we shoot backward with this initial data from $z = L$ to $z = 0$.

Introducing the new space variable $\zeta = L - z$, this backward shooting consists in solving the Cauchy problem

$$(\mathcal{Q}_\theta^b) \begin{cases} V_\theta'(\zeta) = A V_\theta(\zeta) - F(V_\theta(\zeta)) & \forall \zeta \in]0, L[& (39a) \\ v_{\theta,1}(\zeta = 0) = \theta & & (39b) \\ v_{\theta,2}(\zeta = 0) = P_p^{\text{in}} & & (39c) \end{cases}$$

where $\theta = \theta_1 \stackrel{\text{def}}{=} u_{\lambda,1}^{(1)}(L)$. This time, we can expect that $u_{\theta_1,1}^{(2)}(0) = v_{\theta_1,1}(L) = P_p^{\text{in}}$ but there will be limited chances to happen. So, we iterate the process and solve again Cauchy problem (\mathcal{Q}_λ) for $\lambda = u_{\theta_1,2}^{(2)}(0)$ and then the backward Cauchy problem (\mathcal{Q}_θ^b) for $\theta = u_{\lambda,1}^{(2)}(L)$, and so forth until converge of the process occurs.

The Shooting method variant can be interpreted as follows. Since the value $y_2(z = 0)$ is unknown, a first guess λ_1 is chosen and the Cauchy problem deduced from the boundary problem (34) with this guess is solved, *i.e.* the initial data $(P_s^{\text{in}}, \lambda_1)$ is propagated or shoot. Of course, It is quite unlikely that this solution matches the boundary condition $y_2(z = L) = P_p^{\text{in}}$, *i.e.* that the shot reaches the target. So we note the angle of incidence θ_1 of this shot and we move to the target from where we shoot back with the same angle of incidence θ_1 . The projectile goes back to the starting point direction. He will probably miss the starting point

since the angle of incidence θ_1 is not the one of the exact trajectory connecting the two points (starting point and target). Nevertheless, we note the angle of incidence λ_2 of this backward shot and shoot again with the same angle of incidence λ_2 , and so on until the target is reached, that is to say until the good trajectory between the starting point and the target is found.

The principle of the Shooting method is illustrated in Fig. 3.

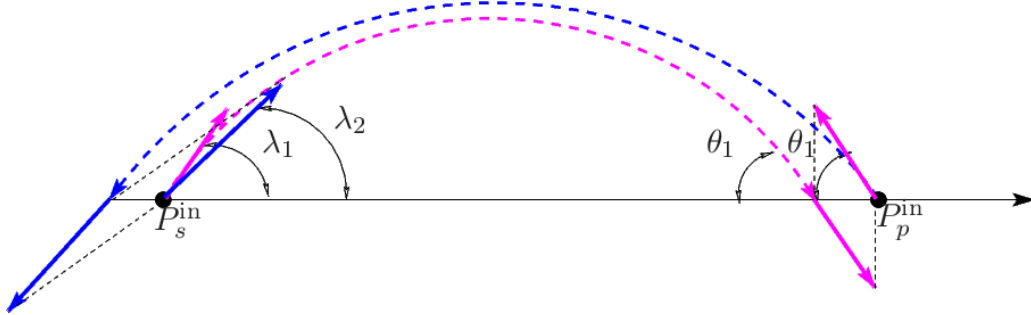


Figure 3: Illustration of the principle of the Shooting method variant.

3.4 The Relaxation method

3.4.1 General considerations

In the contra-propagative case, for a given value of $t \in \mathbb{R}^+$ considered as a parameter, we have to solve the non-linear system of ODE

$$Y_t'(z) = F(Y_t(z)) - A Y_t(z) \stackrel{\text{def}}{=} G(Y_t(z)) \quad \forall z \in [0, L] \quad (40)$$

where the unknown function Y_t is defined as

$$Y_t : z \in [0, L] \mapsto \begin{pmatrix} Y_{t,1}(z) \\ Y_{t,2}(z) \end{pmatrix} \stackrel{\text{def}}{=} \begin{pmatrix} P_s(z, t) \\ P_p(z, t) \end{pmatrix} \in \mathbb{R}^2, \quad (41)$$

and where the 2×2 diagonal matrix with diagonal and the mapping F are defined in (31). This system has to be solved with the boundary conditions

$$Y_{t,1}(0) = P_s^{\text{in}}(t) \quad \text{and} \quad Y_{t,2}(L) = P_p^{\text{in}}(t). \quad (42)$$

From now on, for conciseness, we will omit the parameter t and Y_t will be denoted Y .

To solve (40)–(42), let us introduce a subdivision $(z_k)_{k=0, \dots, K}$ of the interval $[0, L]$ corresponding to the fiber. Let us consider a sub-interval $[z_k, z_{k+1}]$ for $k \in \{0, \dots, K-1\}$. We denote by $h_k = z_{k+1} - z_k$ its length and by Y_k the approximation of Y at node z_k for $k \in \{0, \dots, K\}$. We can approach equation (40) in $[z_k, z_{k+1}]$ by a standard numerical scheme for an ODE system such as Runge-Kutta scheme for instance. We will refer to this scheme as *Method A*. Here are some classical choices for *Method A* and the way Y_k is computed by recurrence.

- When using Euler method (also known as Runge-Kutta scheme RK₁), we obtain the following recurrence relation

$$\begin{aligned} Y_{k+1} &= Y_k + h_k G(Y_k) \\ &= Y_k + h_k \left(F(Y_k) - A Y_k \right) \end{aligned} \quad (43)$$

- When using the forward midpoint method (also known as Runge-Kutta scheme RK₂), we obtain the following recurrence relation

$$\begin{aligned} Y_{k+1} &= Y_k + h_k G\left(Y_k + \frac{h_k}{2} G(Y_k)\right) \\ &= Y_k + h_k K_2 \end{aligned} \quad (44)$$

where

$$\begin{cases} K_1 = F(Y_k) - A Y_k \\ K_2 = F(Y_k + \frac{h_k}{2} K_1) - A (Y_k + \frac{h_k}{2} K_1) \end{cases}$$

- When using the backward midpoint method (an implicit method, the most simple collocation method), we obtain the following recurrence relation

$$\begin{aligned} Y_{k+1} &= Y_k + h_k G\left(\frac{1}{2}(Y_k + Y_{k+1})\right) \\ &= Y_k + h_k \left(F\left(\frac{1}{2}(Y_k + Y_{k+1})\right) - A \frac{1}{2}(Y_k + Y_{k+1}) \right) \end{aligned} \quad (45)$$

- When using the fourth order Runge-Kutta scheme RK₄, we obtain the following recurrence relation

$$Y_{k+1} = Y_k + \frac{h_k}{6} (K_1 + 2K_2 + 2K_3 + K_4) \quad (46)$$

where

$$\begin{cases} K_1 = G(Y_k) = F(Y_k) - A Y_k \\ K_2 = G(Y_k + \frac{h_k}{2} K_1) = F(Y_k + \frac{h_k}{2} K_1) - A (Y_k + \frac{h_k}{2} K_1) \\ K_3 = G(Y_k + \frac{h_k}{2} K_2) = F(Y_k + \frac{h_k}{2} K_2) - A (Y_k + \frac{h_k}{2} K_2) \\ K_4 = G(Y_k + h_k K_3) = F(Y_k + h_k K_3) - A (Y_k + h_k K_3) \end{cases}$$

Note that for the various Runge-Kutta schemes quoted above, we have a relation in the form

$$Y_{k+1} - Y_k - h_k \Psi(Y_k) = 0, \quad \forall k = 0, \dots, K-1 \quad (47)$$

whereas when using the backward midpoint method, we have a relation in the form

$$Y_{k+1} - Y_k - h_k \Psi(Y_{k+1}, Y_k) = 0, \quad \forall k = 0, \dots, K-1. \quad (48)$$

From the boundary conditions, we have

$$Y_0 = \begin{pmatrix} P_s^{\text{in}}(t) \\ Y_{0,2} \end{pmatrix} \quad \text{and} \quad Y_K = \begin{pmatrix} Y_{K,1} \\ P_p^{\text{in}}(t) \end{pmatrix} \quad (49)$$

Finally, equation (47) (resp. (48)) with (70) form a non-linear system of $2K$ equations with $2K$ unknowns: $Y_{0,2}, Y_{K,1}$ and $Y_{k,1}, Y_{k,2}$ for $k = \{1, \dots, K-1\}$. We will only consider in the following the case of the Runge-Kutta schemes where the non-linear system reads, with the notations introduced above,

$$\begin{cases} Y_1 - Y_0 - h_0 \Psi(Y_0) = 0 \\ Y_{k+1} - Y_k - h_k \Psi(Y_k) = 0, \quad \forall k = 1, \dots, K-2 \\ Y_K - Y_{K-1} - h_{K-1} \Psi(Y_{K-1}) = 0 \end{cases} \quad (50)$$

At this stage, we have to chose a numerical method to solve the non-linear system (50). We will refer to this choice of numerical method as *Method B*. Among the classical methods for solving a non-linear system of equations are Newton-Raphson method and the Secant method.

In order to introduce these two methods (and latter on in order to implement these methods in a computer program), we recast the non-linear system (50) as

$$H(\mathbb{Y}) = 0 \quad (51)$$

where the unknown \mathbb{Y} is defined as

$$\begin{aligned} \mathbb{Y} &= (Y_{0,2} \ Y_{1,1} \ Y_{1,2} \ \dots \ Y_{K-1,1} \ Y_{K-1,2} \ Y_{K,1})^\top \\ &\stackrel{\text{def}}{=} (\mathbb{Y}_1 \ \mathbb{Y}_2 \ \mathbb{Y}_3 \ \dots \ \mathbb{Y}_{2K-2} \ \mathbb{Y}_{2K-1} \ \mathbb{Y}_{2K})^\top \end{aligned} \quad (52)$$

and where from (50), the mapping $H : \mathbb{R}^{2K} \rightarrow \mathbb{R}^{2K}$ is defined as

$$\begin{aligned} H(\mathbb{Y}) &= \begin{pmatrix} Y_{1,1} - P_s^{\text{in}} - h_0 \Psi_1(P_s^{\text{in}}, Y_{0,2}) \\ Y_{1,2} - Y_{0,2} - h_0 \Psi_2(P_s^{\text{in}}, Y_{0,2}) \\ \vdots \\ Y_{k+1,1} - Y_{k,1} - h_k \Psi_1(Y_{k,1}, Y_{k,2}) \\ Y_{k+1,2} - Y_{k,2} - h_k \Psi_2(Y_{k,1}, Y_{k,2}) \\ \vdots \\ Y_{K,1} - Y_{K-1,1} - h_{K-1} \Psi_1(Y_{K-1,1}, Y_{K-1,2}) \\ P_p^{\text{in}} - Y_{K-1,2} - h_{K-1} \Psi_2(Y_{K-1,1}, Y_{K-1,2}) \end{pmatrix} \\ &= \begin{pmatrix} \mathbb{Y}_2 - P_s^{\text{in}} - h_0 \Psi_1(P_s^{\text{in}}, \mathbb{Y}_1) \\ \mathbb{Y}_3 - \mathbb{Y}_1 - h_0 \Psi_2(P_s^{\text{in}}, \mathbb{Y}_1) \\ \vdots \\ \mathbb{Y}_{2k+2} - \mathbb{Y}_{2k} - h_k \Psi_1(\mathbb{Y}_{2k}, \mathbb{Y}_{2k+1}) \\ \mathbb{Y}_{2k+3} - \mathbb{Y}_{2k+1} - h_k \Psi_2(\mathbb{Y}_{2k}, \mathbb{Y}_{2k+1}) \\ \vdots \\ \mathbb{Y}_{2K} - \mathbb{Y}_{2K-2} - h_{K-1} \Psi_1(\mathbb{Y}_{2K-2}, \mathbb{Y}_{2K-1}) \\ P_p^{\text{in}} - \mathbb{Y}_{2K-1} - h_{K-1} \Psi_2(\mathbb{Y}_{2K-2}, \mathbb{Y}_{2K-1}) \end{pmatrix}. \end{aligned} \quad (53)$$

The expressions of Ψ_1 and Ψ_2 depend on the choice made for *Method A*. For instance, when using the RK2 scheme, we have

$$\Psi_i(\mathbb{Y}_j, \mathbb{Y}_{j+1}) = G_i((\mathbb{Y}_j, \mathbb{Y}_{j+1})^\top) \quad i = 1, 2 \quad (54)$$

where G_i denotes the i -th component of the mapping G defined in (40), whereas when using the RK4 scheme, we have

$$\Psi_i(\mathbb{Y}_j, \mathbb{Y}_{j+1}) = \frac{1}{6} (K_{1,i} + 2K_{2,i} + 2K_{3,i} + K_{4,i}) \quad i = 1, 2 \quad (55)$$

where

$$\begin{cases} K_{1,i} = G_i((\mathbb{Y}_j, \mathbb{Y}_{j+1})^\top) \\ K_{2,i} = G_i((\mathbb{Y}_j + \frac{h_k}{2} K_{1,1}, \mathbb{Y}_{j+1} + \frac{h_k}{2} K_{1,2})^\top) \\ K_{3,i} = G_i((\mathbb{Y}_j + \frac{h_k}{2} K_{2,1}, \mathbb{Y}_{j+1} + \frac{h_k}{2} K_{2,2})^\top) \\ K_{4,i} = G_i((\mathbb{Y}_j + h_k K_{3,1}, \mathbb{Y}_{j+1} + h_k K_{3,2})^\top) \end{cases}$$

Let us now introduce in our context the two choices for the numerical *Method B* for solving the non-linear system (118) that are Newton-Raphson method and the Secant method.

3.4.2 Newton-Raphson method

The more natural choice for a numerical method for solving the non-linear system (118) is Newton-Raphson method. Starting from an initial guess $\mathbb{Y}^{(0)}$, Newton-Raphson method defines a sequence $(\mathbb{Y}^{(n)})_{n \in \mathbb{N}}$ such that

$$\mathbb{Y}^{(n)} = \mathbb{Y}^{(n-1)} + \delta^{(n-1)} \quad \forall n \geq 1 \quad (56)$$

where $\delta^{(n)}$ denotes the solution to the linear system

$$J_H(\mathbb{Y}^{(n-1)}) \delta^{(n-1)} = -H(\mathbb{Y}^{(n-1)}) \quad (57)$$

where Ψ_1 and Ψ_2 denote the two components of the mapping $\Psi : \mathbb{R}^2 \rightarrow \mathbb{R}^2$ introduced in (47). When considering the RK2 method, the expression of Ψ is given by (44). From the chain rule, we obtain

$$\begin{aligned} \frac{\partial \Psi_1}{\partial \mathbb{Y}_{2k}}(\mathbb{Y}_{2k}, \mathbb{Y}_{2k+1}) &= \left(1 + \frac{h_k}{2} \partial_1 G_1(\mathbb{Y}_{2k}, \mathbb{Y}_{2k+1})\right) \partial_1 G_1(Z_1, Z_2) \\ &\quad + \frac{h_k}{2} \partial_1 G_2(\mathbb{Y}_{2k}, \mathbb{Y}_{2k+1}) \partial_2 G_1(Z_1, Z_2) \end{aligned} \quad (61a)$$

$$\begin{aligned} \frac{\partial \Psi_1}{\partial \mathbb{Y}_{2k+1}}(\mathbb{Y}_{2k}, \mathbb{Y}_{2k+1}) &= \left(1 + \frac{h_k}{2} \partial_2 G_2(\mathbb{Y}_{2k}, \mathbb{Y}_{2k+1})\right) \partial_2 G_1(Z_1, Z_2) \\ &\quad + \frac{h_k}{2} \partial_2 G_1(\mathbb{Y}_{2k}, \mathbb{Y}_{2k+1}) \partial_1 G_1(Z_1, Z_2) \end{aligned} \quad (61b)$$

$$\begin{aligned} \frac{\partial \Psi_2}{\partial \mathbb{Y}_{2k}}(\mathbb{Y}_{2k}, \mathbb{Y}_{2k+1}) &= \left(1 + \frac{h_k}{2} \partial_1 G_1(\mathbb{Y}_{2k}, \mathbb{Y}_{2k+1})\right) \partial_1 G_2(Z_1, Z_2) \\ &\quad + \frac{h_k}{2} \partial_1 G_1(\mathbb{Y}_{2k}, \mathbb{Y}_{2k+1}) \partial_2 G_2(Z_1, Z_2) \end{aligned} \quad (61c)$$

$$\begin{aligned} \frac{\partial \Psi_2}{\partial \mathbb{Y}_{2k+1}}(\mathbb{Y}_{2k}, \mathbb{Y}_{2k+1}) &= \left(1 + \frac{h_k}{2} \partial_2 G_2(\mathbb{Y}_{2k}, \mathbb{Y}_{2k+1})\right) \partial_2 G_2(Z_1, Z_2) \\ &\quad + \frac{h_k}{2} \partial_2 G_1(\mathbb{Y}_{2k}, \mathbb{Y}_{2k+1}) \partial_1 G_2(Z_1, Z_2) \end{aligned} \quad (61d)$$

where

$$\begin{aligned} Z_1 &= \mathbb{Y}_{2k} + \frac{1}{2} h_k G_1(\mathbb{Y}_{2k}, \mathbb{Y}_{2k+1}) \\ Z_2 &= \mathbb{Y}_{2k+1} + \frac{1}{2} h_k G_2(\mathbb{Y}_{2k}, \mathbb{Y}_{2k+1}) \end{aligned}$$

Finally, from (40), we have

$$\begin{aligned} \partial_1 G_1(Z_1, Z_2) &= \partial_1 F_1(Z_1, Z_2) - \alpha_s^{(a)} \\ &= \frac{(2\alpha_s^{(a)} Z_1 + \frac{\nu_s}{\nu_p} \alpha_p^{(a)} Z_2) \left(1 + \frac{Z_1}{P_s^{\text{sat}}} + \frac{Z_2}{P_p^{\text{sat}}}\right) - \frac{1}{P_s^{\text{sat}}} \left(\alpha_s^{(a)} Z_1^2 + \frac{\nu_s}{\nu_p} \alpha_p^{(a)} Z_1 Z_2\right)}{P_s^{\text{sat}} \left(1 + \frac{Z_1}{P_s^{\text{sat}}} + \frac{Z_2}{P_p^{\text{sat}}}\right)^2} - \alpha_s^{(a)} \end{aligned} \quad (62a)$$

$$\begin{aligned} \partial_2 G_1(Z_1, Z_2) &= \partial_2 F_1(Z_1, Z_2) \\ &= \frac{\frac{\nu_s}{\nu_p} \alpha_p^{(a)} Z_1 \left(1 + \frac{Z_1}{P_s^{\text{sat}}} + \frac{Z_2}{P_p^{\text{sat}}}\right) - \frac{1}{P_p^{\text{sat}}} \left(\alpha_s^{(a)} Z_1^2 + \frac{\nu_s}{\nu_p} \alpha_p^{(a)} Z_1 Z_2\right)}{P_s^{\text{sat}} \left(1 + \frac{Z_1}{P_s^{\text{sat}}} + \frac{Z_2}{P_p^{\text{sat}}}\right)^2} \end{aligned} \quad (62b)$$

$$\begin{aligned} \partial_1 G_2(Z_1, Z_2) &= \partial_1 F_2(Z_1, Z_2) \\ &= \frac{\frac{\nu_p}{\nu_s} \alpha_s^{(a)} Z_2 \left(1 + \frac{Z_1}{P_s^{\text{sat}}} + \frac{Z_2}{P_p^{\text{sat}}}\right) - \frac{1}{P_s^{\text{sat}}} \left(\alpha_p^{(a)} Z_2^2 + \frac{\nu_p}{\nu_s} \alpha_s^{(a)} Z_1 Z_2\right)}{u P_p^{\text{sat}} \left(1 + \frac{Z_1}{P_s^{\text{sat}}} + \frac{Z_2}{P_p^{\text{sat}}}\right)^2} \end{aligned} \quad (62c)$$

$$\begin{aligned} \partial_2 G_2(Z_1, Z_2) &= \partial_2 F_2(Z_1, Z_2) - u \alpha_p^{(a)} \\ &= \frac{(2\alpha_p^{(a)} Z_2 + \frac{\nu_p}{\nu_s} \alpha_s^{(a)} Z_1) \left(1 + \frac{Z_1}{P_s^{\text{sat}}} + \frac{Z_2}{P_p^{\text{sat}}}\right) - \frac{1}{P_p^{\text{sat}}} \left(\alpha_p^{(a)} Z_2^2 + \frac{\nu_p}{\nu_s} \alpha_s^{(a)} Z_1 Z_2\right)}{u P_p^{\text{sat}} \left(1 + \frac{Z_1}{P_s^{\text{sat}}} + \frac{Z_2}{P_p^{\text{sat}}}\right)^2} - u \alpha_p^{(a)} \end{aligned} \quad (62d)$$

Combining (62) with (61), we deduce a closed-form expression for the non-zero Jacobian matrix coefficients as defined in (60). Note that although a similar computation could be done with the Runge-Kutta RK4 method, this would be much more tedious to obtain a closed-form expression for the non-zero Jacobian matrix coefficients.

3.4.3 The Secant method

Depending on the choice of the numerical scheme for the ODE, the expression of Ψ can be more or less complicated and therefore a closed-form expression for the Jacobian matrix $J_H(\mathbb{Y})$ can

be more or less easy to obtain. To overcome this difficulty, one can replace the Jacobian matrix $J_H(\mathbb{Y}^{(n-1)})$ involved in the linear system (122) by an approximation. For instance, the Secant method for non-linear systems (also termed Broyden method) consists in solving instead of (122) the linear system

$$Q^{(n-1)} \delta^{(n-1)} = -H(\mathbb{Y}^{(n-1)}) \quad (63)$$

where the sequence of matrix $(Q^{(n)})_{n \in \mathbb{N}}$ is obtained by the recurrence relation

$$Q^{(n)} = Q^{(n-1)} + \frac{V^{(n-1)} (\delta^{(n-1)})^\top}{(\delta^{(n-1)})^\top \delta^{(n-1)}} \quad (64)$$

where $V^{(n-1)}$ is the vector of \mathbb{R}^{2K} defined by

$$V^{(n-1)} = H(\mathbb{Y}^{(n)}) - H(\mathbb{Y}^{(n-1)}) - Q^{(n-1)} \delta^{(n-1)}. \quad (65)$$

Remark. A drawback of the Secant method that can be deduced from (64) is that the matrix $Q^{(n)}$ would be most likely to be full and not sparse as the Jacobian matrix J_H defined in (124).

The Secant method requires the initialization of $Q^{(0)}$. This can be achieved by considering an approximation of $J_H(\mathbb{Y}^{(0)})$ based on a finite difference formula such as

$$(Q^{(0)})_{i,j} = \frac{H_i(\mathbb{Y}^{(0)} + h\mathbf{e}_j) - H_i(\mathbb{Y}^{(0)})}{h} \quad (66)$$

where a first order finite difference was used. The finite difference step-size h must be chosen small enough but not too small to avoid round-off error and poor accuracy. One could also use the second order of accuracy finite difference

$$(Q^{(0)})_{i,j} = \frac{H_i(\mathbb{Y}^{(0)} + h\mathbf{e}_j) - H_i(\mathbb{Y}^{(0)} - h\mathbf{e}_j)}{2h} \quad (67)$$

The algorithm for the Secant method is therefore the following.

1. Choose the initial vector $\mathbb{Y}^{(n=0)}$.
2. Compute the initial matrix Q_0 by formula (66) or (67) for an arbitrary step h chosen small enough but not too small.
3. Solve the linear system $Q_{n=0} \delta^{(n=0)} = -H(\mathbb{Y}^{(n=0)})$.
4. Let $\mathbb{Y}^{(n+1)} = \mathbb{Y}^{(n=0)} + \delta^{(n=0)}$
5. While the stopping criterium is not fulfilled do
 - (a) Compute $b = H(\mathbb{Y}^{(n+1)}) - H(\mathbb{Y}^{(n)})$
 - (b) Compute $Q_{n+1} = Q_n - \frac{(b - Q_n \delta^{(n)}) (\delta^{(n)})^\top}{(\delta^{(n)})^\top \delta^{(n)}}$
 - (c) Solve the linear system $Q_{n+1} \delta^{(n+1)} = -H(\mathbb{Y}^{(n+1)})$
 - (d) Update the variables
 - i. $\mathbb{Y}^{(n)} \leftarrow \mathbb{Y}^{(n+1)}$
 - ii. $\mathbb{Y}^{(n+1)} \leftarrow \mathbb{Y}^{(n+1)} + \delta^{(n+1)}$
 - iii. $Q_{n+1} \leftarrow Q_n$

end do

3.4.4 Choice of Method C for solving the linear system (122)

As mentioned earlier, when choosing the RK2 method as *Method A*, we can obtain an explicit expression for the Jacobian matrix J_H and, using Newton-Raphson method as *Method B* leads us to solve the linear system (122) at each iteration of Newton-Raphson algorithm.

Because of the very special shape of the matrix $J_H(\mathbb{Y}^{(n-1)})$ of the linear system (122) its solution can be computed at a much lower cost than the cost of the standard Gaussian method (whose cost is comparable to $\frac{1}{3}(2K)^3$).

Let us detail a cost-less hand-made algorithm for solving a linear system in the form

$$J_H(\mathbb{Y}^{(n-1)}) X = b \quad (68)$$

where $b \in \mathbb{R}^{2K}$ is the given right-hand side of the linear system and $X \in \mathbb{R}^{2K}$ denotes the unknown. We denote by $J_{i,j}$ the generic element of the matrix $J_H(\mathbb{Y}^{(n-1)})$ ($i, j = 1, \dots, 2K$) and by b_i (resp. X_i) the components of the vector b (resp. X).

The first two equations ($k = 0$) of the linear system (68) read

$$\begin{aligned} J_{1,1} X_1 + X_2 &= b_1 \\ J_{2,1} X_1 + X_3 &= b_2 \end{aligned}$$

It follows that

$$\begin{aligned} X_2 &= S(2) X_1 + T(2) \\ X_3 &= S(3) X_1 + T(3) \end{aligned}$$

where $S(2) = -J_{1,1}$, $T(2) = b_1$, $S(3) = -J_{2,1}$, $T(3) = b_2$.

Let us now assume that we have the expression of X_{2k} and X_{2k+1} in the form

$$X_{2k} = S(2k) X_1 + T(2k) \quad (69a)$$

$$X_{2k+1} = S(2k+1) X_1 + T(2k+1) \quad (69b)$$

Then, equations $2k+1$ and $2k+2$ that read

$$\begin{aligned} J_{2k+1,2k} X_{2k} + J_{2k+1,2k+1} X_{2k+1} + X_{2k+2} &= b_{2k+1} \\ J_{2k+2,2k} X_{2k} + J_{2k+2,2k+1} X_{2k+1} + X_{2k+3} &= b_{2k+2} \end{aligned}$$

we deduce that

$$X_{2k+2} = b_{2k+1} - J_{2k+1,2k} X_{2k} - J_{2k+1,2k+1} X_{2k+1} = S(2k+2) X_1 + T(2k+2)$$

$$X_{2k+3} = b_{2k+2} - J_{2k+2,2k} X_{2k} - J_{2k+2,2k+1} X_{2k+1} = S(2k+3) X_1 + T(2k+3)$$

where

$$S(2k+2) = -J_{2k+1,2k} S(2k) - J_{2k+1,2k+1} S(2k+1) \quad (70a)$$

$$T(2k+2) = b_{2k+1} - J_{2k+1,2k} T_{2k} - J_{2k+1,2k+1} T_{2k+1} \quad (70b)$$

$$S(2k+3) = -J_{2k+2,2k} S(2k) - J_{2k+2,2k+1} S(2k+1) \quad (70c)$$

$$T(2k+3) = b_{2k+2} - J_{2k+2,2k} T_{2k} - J_{2k+2,2k+1} T_{2k+1} \quad (70d)$$

The last two equations read

$$J_{2K-1,2K-2} X_{2K-2} + J_{2K-1,2K-1} X_{2K-1} + X_{2K} = b_{2K-1} \quad (71a)$$

$$J_{2K,2K-2} X_{2K-2} + J_{2K,2K-1} X_{2K-1} = b_{2K} \quad (71b)$$

From (71b), we deduce that

$$J_{2K,2K-2} (S(2K-2) X_1 + T(2K-2)) + J_{2K,2K-1} (S(2K-1) X_1 + T(2K-1)) = b_{2K} \quad (72)$$

and this last equation can be solved for X_1 . We obtain

$$X_1 = \frac{b_{2K} - T(2K-2) - T(2K-1)}{J_{2K,2K-2} S(2K-2) + J_{2K,2K-1} S(2K-1)} \quad (73)$$

Once X_1 is known, we obtain the other components of the solution X by relations (69a) for $k = 1, \dots, K-1$ and X_{2K} is obtained from (71a).

Let us examine the cost of this algorithm. First, we have to compute by induction the coefficients $S(2k), S(2k+1), T(2k), T(2k+1)$ for k from 2 to $K-1$ using relations (70). The cost is $8(K-1)$ multiplications and $6(K-1)$ additions. Then to compute X_1 and X_{2K} , we have 5 multiplications/divisions and 6 additions. Finally, to compute the other components of X by relations (69a) for $k = 1, \dots, K-1$ we have $2(K-1)$ multiplications and $2(K-1)$ additions. The total cost is therefore $10(K-1) + 5$ multiplications and $8(K-1) + 6$ additions. The cost of this algorithm is therefore proportional to $10K$ and thus it is linear with the number of grid points K . (Whereas the cost of Gaussian elimination is proportional to $\frac{1}{3}K^3$.)

3.5 Numerical illustration

We have considered a Erbium fiber amplifier with the following properties:

- Fiber length $L = 10$ m
- Erbium ions density $N = 1.4 \cdot 10^{25} \text{ m}^{-3}$
- $\Gamma_p = 0.88$
- $\Gamma_s = 0.52$
- $A_{\text{eff}} = 8.043 \cdot 10^{-12} \text{ m}^2$
- $\alpha_p^{(a)} = 1.3816 \cdot 10^{-3} \text{ m}^{-1}$
- $\alpha_s^{(a)} = 1.3816 \cdot 10^{-3} \text{ m}^{-1}$
- Metastable level 2 lifetime $\tau_2 = 10^{-2} \text{ s}$
- $\sigma_p^{(a)} = 2.113 \cdot 10^{-26} \text{ m}^2$
- $\sigma_p^{(e)} = 0$
- $\sigma_s^{(a)} = 8.6106 \cdot 10^{-26} \text{ m}^2$
- $\sigma_s^{(e)} = 1.4263 \cdot 10^{-26} \text{ m}^2$
- $P_s^{\text{in}} = 10^{-2} \text{ W}$
- $P_p^{\text{in}} = 8 \cdot 10^{-2} \text{ W}$

Computation were achieved on a laptop personal computer (Intel Core i5, 8 Go RAM) under Linux Ubuntu operating system.

3.5.1 Using the Shooting methods

In the co-propagating case, the pump and signal powers along the fiber are depicted in Fig. 4. The Cauchy problem formed by the non-linear ODE system (29) with boundary conditions (107) was solved under MATLAB using a Runge-Kutta RK4(5) scheme (ode45 solver). The computational time (CPU time) was 0.02 s.

To validate the computation we have compared the total output power to the value obtained when solving the non-linear equation (27) (under MATLAB using the `fsolve` solver). The results are as follows:

CPU Time = 0.02 s.

Comparison of the value of the total power out :

By solving the nonlinear ODE systeme $P_{out} = 0.075367$

By solving the nonlinear equ. $P_{out} = 0.075367$

Relative error = $2.0623e-14$

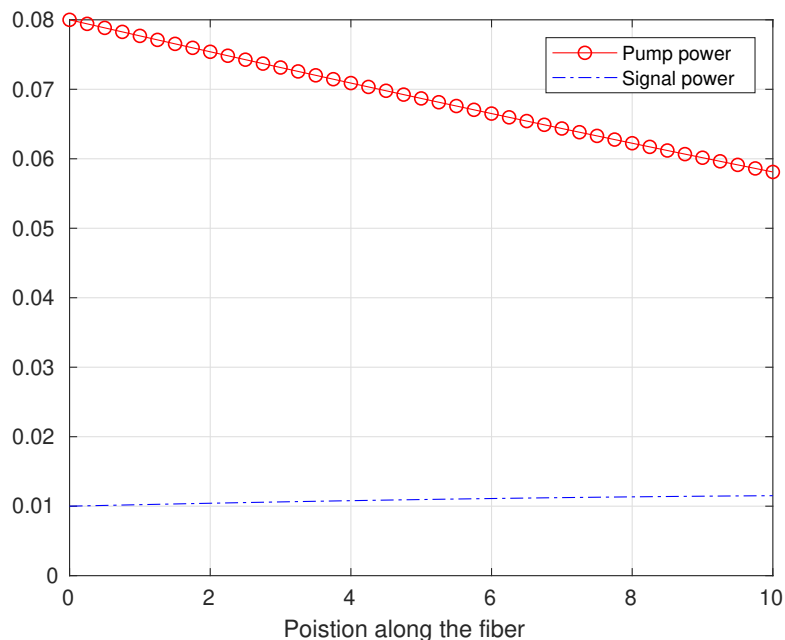


Figure 4: The co-propagative case.

In the contra-propagating case, the pump and signal powers along the fiber are depicted in Fig. 5. The boundary value problem formed by the non-linear ODE system (29) with boundary conditions (109) was solved under MATLAB using the shooting method described in the previous section. It is worthily to notice that the Secant method converges with only seven iterations. The computational time (CPU time) was 0.06 s. The method is accurate: We have compared the total output power to the value obtained when solving the non-linear equation (27) (under MATLAB using the `fsolve` solver). The results are as follows:

Iterate 3 - Root approx = 0.058992 - Value of the function = 0.0010291

Iterate 4 - Root approx = 0.058064 - Value of the function = $-4.2842e-05$

Iterate 5 - Root approx = 0.058101 - Value of the function = $3.766e-08$

Iterate 6 - Root approx = 0.058101 - Value of the function = $1.3869e-12$

Iterate 7 - Root approx = 0.058101 - Value of the function = $-1.3878e-17$

CPU Time = 0.06 s.

Comparison of the value of the total power out :
 By solving the nonlinear ODE systeme $P_{out} = 0.075367$
 By solving the nonlinear equ. $P_{out} = 0.075367$
 Relative error = $1.4363e-13$

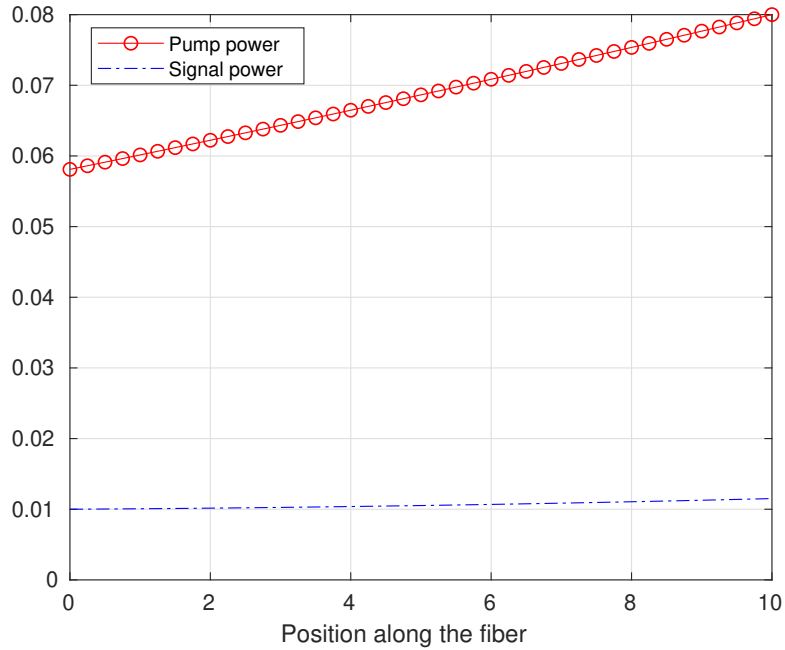


Figure 5: The contra-propagative case.

We have also use the second Shooting method described in Section 3.3. to compute the pump and source powers in the contra-propagating case. We obtained an accurate solution after 7 round trips and a last solving of the forward problem, that is to say after 15 solving of a Cauchy problem by MATLAB ode45 solver. The computation time (CPU time) was 0.03 s.

```
>> main_contrapropag_shooting_laas
CPU Time = 0.03 s.
Number of iterations = 15
Comparison of the value of the total power out :
By solving the nonlinear ODE systeme  $P_{out} = 0.075367$ 
By solving the nonlinear equ.  $P_{out} = 0.075367$ 
Relative error =  $4.9717e-14$ 
```

3.5.2 Using the Relaxation approach

We have compared various Relaxation approaches to solve the contra-propagating problem.

- RK2 + Newton-Raphson + our specific algorithm

The first Relaxation approach we have tested uses the RK2 scheme as *Method A*, Newton-Raphson method as *Method B* and our specific algorithm introduced in Section 3.4.4 to solve the linear system (122). We have made simulations for the following values of K : $K = 10$, $K = 100$ and $K = 1000$ and here again we have compared the total output power to the value obtained when solving the non-linear equation (27) (under MATLAB using the `fsolve` solver). Results are as follows:

```

>> main_newton
Number of sub-intervals in the subdivision of [0,L] = 10
CPU time of the simulation = 0.03 s.
Number of iteration of Newton-Raphson method = 7
  Comparison of the value of the total power out :
  By solving the nonlinear ODE systeme P_out = 0.075367
  By solving the nonlinear equ. P_out = 0.075367
  Relative error = 3.7114e-07

>> main_newton
Number of sub-intervals in the subdivision of [0,L] = 100
CPU time of the simulation = 0.04 s.
Number of iteration of Newton-Raphson method = 6
  Comparison of the value of the total power out :
  By solving the nonlinear ODE systeme P_out = 0.075367
  By solving the nonlinear equ. P_out = 0.075367
  Relative error = 3.6866e-09

>> main_newton
Number of sub-intervals in the subdivision of [0,L] = 1000
CPU time of the simulation = 0.47 s.
Number of iteration of Newton-Raphson method = 5
  Comparison of the value of the total power out :
  By solving the nonlinear ODE systeme P_out = 0.075367
  By solving the nonlinear equ. P_out = 0.075367
  Relative error = 3.6843e-11

```

One can notice that the error is divided by 10^2 when K is multiplied by 10 as expected since the RK2 scheme is second order accurate. We would like to point out that the Jacobian matrix is stored in a full storage since we have observed that using MATLAB sparse storage increases the computation time. For instance, when $K = 1000$, computation time is 0.75 s. when using the sparse storage whereas it is 0.47 s. using a full storage. However, memory space available quickly becomes a limitation when K increases when the Jacobian matrix is stored in a full storage.

To obtain the same accuracy as the one obtained with the Shooting method (a relative error closed to 10^{-13}), we must chose $K = 10^4$ and the computational time increases to 4.67 s. for this Relaxation method compared to 0.06 s. for the Shooting method (roughly speaking a hundred time more).

```

>> main_newton
Number of sub-intervals in the subdivision of [0,L] = 10000
CPU time of the simulation = 4.67 s.
Number of iteration of Newton-Raphson method = 5
  Comparison of the value of the total power out :
  By solving the nonlinear ODE systeme P_out = 0.075367
  By solving the nonlinear equ. P_out = 0.075367
  Relative error = 3.6919e-13

```

- RK2 + Newton-Raphson + MATLAB mldivide

In order to evaluate the gain in efficiency provided by our specific algorithm introduced in Section 3.4.4 to solve the linear system (122), we have compared the previous results for the

solving of the contra-propagating problem to a simulation with the linear system (122) solved by MATLAB mldivide routine.

When a full storage for the Jacobian matrix is used, for $K = 10^3$, the CPU time when using MATLAB mldivide routine is 1.97 s. (to be compared to 0.47 s. when our specific algorithm is used). However, when a sparse storage for the Jacobian matrix is used, for $K = 10^3$, the CPU time when using MATLAB mldivide routine falls to 0.26 s. This surprising results (our specific algorithm is optimized for the Jacobian matrix we have) can be explained by the fact that MATLAB mldivide routine is probably implemented in the MATLAB kernel whereas our specific algorithm is provided in the MATLAB interpreted language (and must therefore be translated before execution (on the contrary to MATLAB mldivide routine)).

- RK4+ Secant+ MATLAB mldivide

When *Method A* used to discretized the non-linear ODE system is the RK4 scheme, as explained before it is a very hard job to obtain an explicit expression for the Jacobian matrix J_H . This difficulty can be overcome by using the Secant method rather than Newton-Raphson method. In the Secant method, approximations of the Jacobian matrix J_H are computed, and these approximations only require the expression of H . However, one should be aware of the fact that these approximations of the Jacobian matrix J_H are not anymore sparse matrices. As a consequence, it is not possible to use our specific algorithm introduced in Section 3.4.4 to solve the linear system (63) anymore and Gaussian elimination algorithm is used (through MATLAB mldivide routine). This induces an important increase of the computation time compensated however by the fact that to reach a given accuracy, the size of the linear system ($2K$) is much lower when using the RK4 scheme than when using the RK2 method.

For instance an accuracy of 10^{-14} is reached when using the RK4 scheme for a discretization of the fiber length in $K = 100$ sub-intervals whereas the same accuracy with the RK2 scheme requires to have $K \approx 1000$.

```
>> main_secante
RK4 scheme
CPU time of the simulation = 0.53 s.
Number of iteration of the Secant method = 6
Comparison of the value of the total power out :
By solving the nonlinear ODE systeme P_out = 0.075367
By solving the nonlinear equ. P_out = 0.075367
Relative error = 2.2833e-14
```

- RK2+ Secant+ MATLAB mldivide

For comprehensiveness, we have made simulations using a discretization of the non-linear ODE system by the RK2 scheme and a solving of the resulting non-linear system by the Secant method. The results are reported below.

```
>> main_secante
rk2 method
Number of sub-intervals in the subdivision of [0,L] = 10
CPU time of the simulation = 0.03 s.
Number of iteration of the Secant method = 6
Comparison of the value of the total power out :
By solving the nonlinear ODE systeme P_out = 0.075367
By solving the nonlinear equ. P_out = 0.075367
Relative error = 3.7114e-07
```

```

>> main_secante
rk2 method
Number of sub-intervals in the subdivision of [0,L] = 100
CPU time of the simulation = 0.49 s.
Number of iteration of the Secant method = 6
Comparison of the value of the total power out :
By solving the nonlinear ODE systeme P_out = 0.075367
By solving the nonlinear equ. P_out = 0.075367
Relative error = 3.6866e-09

>> main_secante
rk2 method
Number of sub-intervals in the subdivision of [0,L] = 1000
CPU time of the simulation = 19.7 s.
Number of iteration of the Secant method = 6
Comparison of the value of the total power out :
By solving the nonlinear ODE systeme P_out = 0.075367
By solving the nonlinear equ. P_out = 0.075367
Relative error = 3.6843e-11

```

One can observe that the method is second order accurate as expected: increasing the number of subdivision steps by 10 results in a decrease of the error by a factor 100.

In conclusion, for solving the contra-propagative problem with the simple model without ASE, our numerical experiments have shown that the most efficient method is the Shooting method.

4 A model including amplified spontaneous emission

4.1 The model

The treatment outlined in the previous sections neglects an important factor present in all optical amplifiers, that of spontaneous emission. All the excited ions can spontaneously relax from the upper state to the ground state by emitting a photon that is uncorrelated with the signal photons. This spontaneously emitted photon can be amplified as it travels down the fiber and stimulates the emission of more photons from excited ions, photons that belong to the same mode of the electromagnetic field as the original spontaneous photon. This parasitic process, which can occur at any frequency within the fluorescence spectrum of the amplifier transitions, obviously reduces the gain from the amplifier. It robs photons that would otherwise participate in stimulated emission with the signal photons. It is usually referred to as ASE (amplified spontaneous emission). Ultimately, it limits the total amount of gain available from the amplifier.

The total ASE power at a point z along the fiber is the sum of the ASE power from the other locations along the fiber and the added local noise power P_A^0 (corresponding to the spontaneous emission power at the given point z). For a single transverse mode fiber with two independent polarizations for a given mode at frequency ν , the noise power in a bandwidth $\delta\nu$ corresponding to spontaneous emission, is equal to

$$P_A^0(\nu) = 2h\nu\delta\nu. \quad (74)$$

This local noise power will stimulate the emission of photons from excited erbium ions, proportionally to the product $\sigma^{(e)}(\nu) N_2(z)$, where $\sigma^{(e)}(\nu)$ is the stimulated emission cross section at frequency ν . The propagation equation for the ASE power propagating in a given direction is thus

$$\frac{\partial P_A}{\partial z}(z, t, \nu) = \left(N_2(z, t) \sigma^{(e)}(\nu) - N_1(z, t) \sigma^{(a)}(\nu) \right) P_A(z, t, \nu) + P_A^0(\nu) N_2(z, t) \sigma^{(e)}(\nu) \quad (75)$$

where $\sigma^{(a)}(\nu)$ denotes the stimulated absorption cross section at frequency ν .

The modeling of the ASE can be done by dividing the ASE into J small frequency intervals of width $\delta\nu$ much smaller than the transition bandwidth. We denote by ν_1, \dots, ν_J the center of these frequency intervals. The ASE power $P_A(\nu_j)$ within each frequency interval centered in ν_j , $j = 1, \dots, J$, can be considered to propagate as an independent signal. An added complication is that the ASE can actually propagate in both directions along the fiber, both co-propagating and counter-propagating with the pump. Each ASE power $P_A(\nu_j)$ is then decomposed into a forward-traveling ASE component $P_A^+(\nu_j)$ and a backward-traveling ASE component $P_A^-(\nu_j)$ such that

$$P_A(\nu_j) = P_A^+(\nu_j) + P_A^-(\nu_j). \quad (76)$$

In addition to the propagation equations for the pump and signal powers given by (10), we now have for each ASE power $P_A(\nu_j)$ two propagation equations, one for the forward traveling ASE component $P_A^+(\nu_j)$ and one for the backward traveling ASE component $P_A^-(\nu_j)$. We also allow for possible intrinsic background loss in the fiber by means of the parameters $\alpha_p^{(0)}$, $\alpha_s^{(0)}$ and $\alpha_j^{(0)}$. The model is then composed of the following propagation equations for all $z \in [0, L]$ and for all

$t \in \mathbb{R}^+$

$$\left\{ \begin{array}{l} \frac{\partial P_s}{\partial z}(z, t) = \left((\sigma_s^{(e)} + \sigma_s^{(a)}) N_2(z, t) - \sigma_s^{(a)} N \right) \Gamma_s P_s(z, t) - \alpha_s^{(0)} P_s(z, t) \quad (77a) \\ \frac{\partial P_p}{\partial z}(z, t) = u \left((\sigma_p^{(e)} + \sigma_p^{(a)}) N_2(z, t) - \sigma_p^{(a)} N \right) \Gamma_p P_p(z, t) - \alpha_p^{(0)} P_p(z, t) \quad (77b) \\ \frac{\partial P_A^+}{\partial z}(z, t, \nu_j) = \left((\sigma^{(e)}(\nu_j) + \sigma^{(a)}(\nu_j)) N_2(z, t) - \sigma^{(a)}(\nu_j) N \right) \Gamma_s P_A^+(z, t, \nu_j) \\ \quad + \frac{1}{2} P_A^0(\nu_j) \Gamma_s N_2(z, t) \sigma^{(e)}(\nu_j) - \alpha_j^{(0)} P_A^+(z, t, \nu_j) \quad (77c) \\ \frac{\partial P_A^-}{\partial z}(z, t, \nu_j) = - \left((\sigma^{(e)}(\nu_j) + \sigma^{(a)}(\nu_j)) N_2(z, t) - \sigma^{(a)}(\nu_j) N \right) \Gamma_s P_A^-(z, t, \nu_j) \\ \quad - \frac{1}{2} P_A^0(\nu_j) \Gamma_s N_2(z, t) \sigma^{(e)}(\nu_j) + \alpha_j^{(0)} P_A^-(z, t, \nu_j) \quad (77d) \end{array} \right.$$

where the index j ranges from 1 to J and where we have used the notations introduced in Section 3.

Taking into account the ASE, the rate equations (7) now read

$$\left\{ \begin{array}{l} \frac{\partial N_2}{\partial t}(z, t) = -\Gamma_{21} N_2(z, t) + (\sigma_s^{(a)} N_1(z, t) - \sigma_s^{(e)} N_2(z, t)) \phi_s(z, t) \\ \quad + (\sigma_p^{(a)} N_1(z, t) - \sigma_p^{(e)} N_2(z, t)) \phi_p(z, t) \\ \quad + \sum_{j=1}^J (\sigma^{(a)}(\nu_j) N_1(z, t) - \sigma^{(e)}(\nu_j) N_2(z, t)) \phi_A(z, t, \nu_j) \quad (78a) \\ \frac{\partial N_1}{\partial t}(z, t) = \Gamma_{21} N_2(z, t) + (\sigma_s^{(e)} N_2(z, t) - \sigma_s^{(a)} N_1(z, t)) \phi_s(z, t) \\ \quad + (\sigma_p^{(e)} N_2(z, t) - \sigma_p^{(a)} N_1(z, t)) \phi_p(z, t) \\ \quad + \sum_{j=1}^J (\sigma^{(e)}(\nu_j) N_2(z, t) - \sigma^{(a)}(\nu_j) N_1(z, t)) \phi_A(z, t, \nu_j) \quad (78b) \end{array} \right.$$

where for all $j = 1, \dots, J$, $\phi_A(z, t, \nu_j)$ denotes the ASE signal intensity flux at frequency ν_j at position z along the fiber and at time t .

In the steady-state regime, the rate equations (78) can be solved analytically. We have $N = N_1(z, t) + N_2(z, t)$ for all $t \in \mathbb{R}^+$ and we deduce from (78a) that

$$N_2(z, t) = \frac{\sigma_s^{(a)} \phi_s(z, t) + \sigma_p^{(a)} \phi_p(z, t) + \sum_{j=1}^J \sigma^{(a)}(\nu_j) \phi_A(z, t, \nu_j)}{\Gamma_{21} + (\sigma_s^{(a)} + \sigma_s^{(e)}) \phi_s(z, t) + (\sigma_p^{(a)} + \sigma_p^{(e)}) \phi_p(z, t) + \sum_{j=1}^J (\sigma^{(a)}(\nu_j) + \sigma^{(e)}(\nu_j)) \phi_A(z, t, \nu_j)} N \quad (79)$$

Note that this relation coincides with (6.2) in [1].

The expression of the ion population in Level 2 can also be expressed in terms of the field powers. From relations (9), we have

$$\phi_s(z, t) = \frac{\Gamma_s}{h\nu_s A_{\text{eff}}} P_s(z, t), \quad \phi_p(z, t) = \frac{\Gamma_s}{h\nu_p A_{\text{eff}}} P_p(z, t) \quad (80)$$

and

$$\phi_A(z, t, \nu_j) = \frac{\Gamma_j}{h\nu_j A_{\text{eff}}} P_A(z, t, \nu_j) \quad (81)$$

where $P_A = P_A^+ + P_A^-$, A_{eff} is the cross-sectional area of the erbium ion distribution in the fiber, Γ_s (resp. Γ_p and Γ_j) is the overlap factor representing the overlap between the erbium ions and

the mode of the source (resp. pump and ASE) field and P_s (resp. P_p and $P_A(\cdot, \cdot, \nu_j)$) is the signal (resp. pump and ASE) field power. We deduce from (79) that

$$N_2(z, t) = \frac{\tau_2}{A_{\text{eff}}} \frac{\frac{\alpha_p^{(a)}}{h\nu_p} P_p(z, t) + \frac{\alpha_s^{(a)}}{h\nu_s} P_s(z, t) + \sum_{j=1}^J \frac{\alpha_A^{(a)}(\nu_j)}{h\nu_j} P_A(z, t, \nu_j)}{1 + \frac{P_s(z, t)}{P_s^{\text{sat}}} + \frac{P_p(z, t)}{P_p^{\text{sat}}} + \sum_{j=1}^J \frac{P_A(z, t, \nu_j)}{P_A^{\text{sat}}(\nu_j)}} \quad (82)$$

where $\tau_2 = \frac{1}{\Gamma_{21}}$ is the lifetime of level 2, the pump attenuation constant $\alpha_p^{(a)}$ and the signal attenuation constant $\alpha_s^{(a)}$ are defined respectively in (13a) and (13b), the ASE attenuation constants $\alpha_A^{(a)}(\nu_j)$ are given by

$$\alpha_A^{(a)}(\nu_j) = N \Gamma_j \sigma^{(a)}(\nu_j), \quad (83)$$

the saturation powers for the pump and for the signal denoted respectively by P_p^{sat} and P_s^{sat} are defined in (14a) and (14b) and the saturation powers for the ASE signal is given by

$$P_A^{\text{sat}}(\nu_j) = \frac{A_{\text{eff}} \Gamma_{21} h\nu_j}{(\sigma^{(a)}(\nu_j) + \sigma^{(e)}(\nu_j)) \Gamma_j}. \quad (84)$$

The propagation equations (77) then read, for all $z \in [0, L]$ and for all $t \in \mathbb{R}^+$,

$$\left\{ \begin{array}{l} \frac{\partial P_s}{\partial z}(z, t) = G_s[(z, t), P_s, P_p, P_A] \frac{P_s(z, t)}{P_s^{\text{sat}}} - (\alpha_s^{(a)} + \alpha_s^{(0)}) P_s(z, t) \end{array} \right. \quad (85a)$$

$$\left\{ \begin{array}{l} u \frac{\partial P_p}{\partial z}(z, t) = G_p[(z, t), P_s, P_p, P_A] \frac{P_p(z, t)}{P_p^{\text{sat}}} - (\alpha_p^{(a)} + \alpha_p^{(0)}) P_p(z, t) \end{array} \right. \quad (85b)$$

$$\left\{ \begin{array}{l} \frac{\partial P_A^+}{\partial z}(z, t, \nu_j) = \frac{\Gamma_s}{\Gamma_j} G_j[(z, t), P_s, P_p, P_A] \left(\frac{P_A^+(z, t, \nu_j)}{P_A^{\text{sat}}(\nu_j)} + \frac{1}{2} \frac{P_A^0(\nu_j)}{P_A^{\text{sat},(e)}(\nu_j)} \right) \\ \quad - (\alpha_A^{(a)}(\nu_j) + \alpha_A^{(0)}(\nu_j)) P_A^+(z, t, \nu_j) \end{array} \right. \quad (85c)$$

$$\left\{ \begin{array}{l} \frac{\partial P_A^-}{\partial z}(z, t, \nu_j) = -\frac{\Gamma_s}{\Gamma_j} G_j[(z, t), P_s, P_p, P_A] \left(\frac{P_A^-(z, t, \nu_j)}{P_A^{\text{sat}}(\nu_j)} + \frac{1}{2} \frac{P_A^0(\nu_j)}{P_A^{\text{sat},(e)}(\nu_j)} \right) \\ \quad + (\alpha_A^{(a)}(\nu_j) + \alpha_A^{(0)}(\nu_j)) P_A^-(z, t, \nu_j) \end{array} \right. \quad (85d)$$

where the index j ranges from 1 to J and where we have set

$$G_s[(z, t), P_s, P_p, P_A] = \frac{\alpha_s^{(a)} P_s(z, t) + \frac{\nu_s}{\nu_p} \alpha_p^{(a)} P_p(z, t) + \sum_{k=1}^J \frac{\nu_s}{\nu_k} \alpha_A^{(a)}(\nu_k) P_A(z, t, \nu_k)}{1 + \frac{P_s(z, t)}{P_s^{\text{sat}}} + \frac{P_p(z, t)}{P_p^{\text{sat}}} + \sum_{k=1}^J \frac{P_A(z, t, \nu_k)}{P_A^{\text{sat}}(\nu_k)}} \quad (86a)$$

$$G_p[(z, t), P_s, P_p, P_A] = \frac{\frac{\nu_p}{\nu_s} \alpha_s^{(a)} P_s(z, t) + \alpha_p^{(a)} P_p(z, t) + \sum_{k=1}^J \frac{\nu_p}{\nu_k} \alpha_A^{(a)}(\nu_k) P_A(z, t, \nu_k)}{1 + \frac{P_s(z, t)}{P_s^{\text{sat}}} + \frac{P_p(z, t)}{P_p^{\text{sat}}} + \sum_{k=1}^J \frac{P_A(z, t, \nu_k)}{P_A^{\text{sat}}(\nu_k)}} \quad (86b)$$

$$G_j[(z, t), P_s, P_p, P_A] = \frac{\frac{\nu_j}{\nu_s} \alpha_s^{(a)} P_s(z, t) + \frac{\nu_j}{\nu_p} \alpha_p^{(a)} P_p(z, t) + \sum_{k=1}^J \frac{\nu_j}{\nu_k} \alpha_A^{(a)}(\nu_k) P_A(z, t, \nu_k)}{1 + \frac{P_s(z, t)}{P_s^{\text{sat}}} + \frac{P_p(z, t)}{P_p^{\text{sat}}} + \sum_{k=1}^J \frac{P_A(z, t, \nu_k)}{P_A^{\text{sat}}(\nu_k)}} \quad (86c)$$

and

$$P_A^{\text{sat},(e)}(\nu_j) = \frac{A_{\text{eff}} \Gamma_{12} h\nu_j}{\sigma^{(e)}(\nu_j) \Gamma_j}. \quad (87)$$

4.2 Analytical expression of the total output power

Let us denote by P_s^{in} and P_s^{out} the input and output powers of the signal field at the fiber ends $z = 0$ and $z = L$ respectively; Namely $P_s(z = 0, t) = P_s^{\text{in}}(t)$ and $P_s(z = L, t) = P_s^{\text{out}}(t)$ for all

time $t \geq 0$. Similarly, we denote by P_p^{in} and P_p^{out} the input and output powers of the pump field at the fiber ends. If the pump field is co-propagating ($u = +1$), we have $P_p(z = 0, t) = P_p^{\text{in}}(t)$ and $P_p(z = L, t) = P_p^{\text{out}}(t)$ for all time $t \geq 0$ whereas if the pump field is contra-propagating ($u = -1$), we have $P_p(z = L, t) = P_p^{\text{in}}(t)$ and $P_p(z = 0, t) = P_p^{\text{out}}(t)$ for all time $t \geq 0$. Finally, we denote by $P_A^{\text{in}}(\nu_j)$ and $P_A^{\text{out}}(\nu_j)$ the input and output powers of the ASE field for the frequency ν_j at the fiber ends, i.e.

$$P_A^{\text{in}}(\nu_j) = P_A^+(z = 0, \nu_j) + P_A^-(z = L, \nu_j), \quad P_A^{\text{out}}(\nu_j) = P_A^+(z = L, \nu_j) + P_A^-(z = 0, \nu_j).$$

In order to find an analytical expression for the total output power, we make the following assumptions:

(\mathcal{H}_1) The intrinsic background losses in the fiber are zero: $\alpha_p^{(0)} = \alpha_s^{(0)} = \alpha_A^{(0)} = 0$;

(\mathcal{H}_2) The noise power $P_A^{(0)}$ is zero;

(\mathcal{H}_3) The overlap factor Γ_j between the Erbium ions and the mode of the ASE is equal to the overlap factor Γ_s between the Erbium ions and the mode of the source: $\Gamma_j = \Gamma_s$.

In a first step, we consider the sum of equation (85a), equation (85b) multiplied by $\frac{\nu_s}{\nu_p}$, equations (85c) for $j = 1, \dots, J$ multiplied by $\frac{\nu_s}{\nu_j}$ and we subtract the sum of equations (85d) for $j = 1, \dots, J$ multiplied by $\frac{\nu_s}{\nu_j}$. Schematically, we consider

$$(85a) + \frac{\nu_s}{\nu_p} \times (85b) + \sum_{j=1}^J \frac{\nu_s}{\nu_j} \times ((85c) - (85d)).$$

After a tedious calculation, we obtain that G_s defined in (86a) is such that

$$-G_s[(z, t), P_s, P_p, P_A] = \frac{\partial P_s}{\partial z}(z, t) + \frac{\nu_s}{\nu_p} u \frac{\partial P_p}{\partial z}(z, t) + \sum_{j=1}^J \frac{\nu_s}{\nu_j} \left(\frac{\partial P_A^+}{\partial z}(z, t, \nu_j) - \frac{\partial P_A^-}{\partial z}(z, t, \nu_j) \right). \quad (88)$$

In a second step, we consider the sum of equation (85b), equation (85a) multiplied by $\frac{\nu_p}{\nu_s}$, equations (85c) for $j = 1, \dots, J$ multiplied by $\frac{\nu_p}{\nu_j}$ and we subtract the sum of equations (85d) for $j = 1, \dots, J$ multiplied by $\frac{\nu_p}{\nu_j}$. Schematically, we consider

$$(85b) + \frac{\nu_p}{\nu_s} \times (85a) + \sum_{j=1}^J \frac{\nu_p}{\nu_j} \times ((85c) - (85d)).$$

After a new tedious calculation, we obtain that G_p defined in (86b) is such that

$$-G_p[(z, t), P_s, P_p, P_A] = u \frac{\partial P_p}{\partial z}(z, t) + \frac{\nu_p}{\nu_s} \frac{\partial P_s}{\partial z}(z, t) + \sum_{j=1}^J \frac{\nu_p}{\nu_j} \left(\frac{\partial P_A^+}{\partial z}(z, t, \nu_j) - \frac{\partial P_A^-}{\partial z}(z, t, \nu_j) \right). \quad (89)$$

In a last step, we consider the sum of equation (85a) multiplied by $\frac{\nu_k}{\nu_s}$, equation (85b) multiplied by $\frac{\nu_k}{\nu_p}$, equations (85c) for $j = 1, \dots, J$ multiplied by $\frac{\nu_k}{\nu_j}$ and we subtract the sum of equations (85d) for $j = 1, \dots, J$ multiplied by $\frac{\nu_k}{\nu_j}$. Schematically, we consider

$$\frac{\nu_k}{\nu_s} (85a) + \frac{\nu_k}{\nu_p} \times (85b) + \sum_{j=1}^J \frac{\nu_k}{\nu_j} \times ((85c) - (85d))$$

for all $k = 1, \dots, J$. This leads this time to the following relation for G_j defined in (86c)

$$-G_j[(z, t), P_s, P_p, P_A] = \frac{\nu_j}{\nu_s} \frac{\partial P_s}{\partial z}(z, t) + \frac{\nu_j}{\nu_p} u \frac{\partial P_p}{\partial z}(z, t) + \sum_{\ell=1}^J \frac{\nu_j}{\nu_\ell} \left(\frac{\partial P_A^+}{\partial z}(z, t, \nu_\ell) - \frac{\partial P_A^-}{\partial z}(z, t, \nu_\ell) \right). \quad (90)$$

Finally, combining (88), (89) and (90) with (85), taking into account assumptions (\mathcal{H}_1), (\mathcal{H}_2) and (\mathcal{H}_3), we obtain that

$$\left\{ \begin{aligned} \frac{\partial P_s}{\partial z}(z, t) &= - \left(\alpha_s^{(a)} + \frac{1}{P_s^{\text{sat}}} \left(\frac{\partial P_s}{\partial z}(z, t) + \frac{\nu_s}{\nu_p} u \frac{\partial P_p}{\partial z}(z, t) \right. \right. \\ &\quad \left. \left. + \sum_{j=1}^J \frac{\nu_s}{\nu_j} \left(\frac{\partial P_A^+}{\partial z}(z, t, \nu_j) - \frac{\partial P_A^-}{\partial z}(z, t, \nu_j) \right) \right) \right) P_s(z, t) \end{aligned} \right. \quad (91a)$$

$$\left\{ \begin{aligned} u \frac{\partial P_p}{\partial z}(z, t) &= - \left(\alpha_p^{(a)} + \frac{1}{P_p^{\text{sat}}} \left(\frac{\nu_p}{\nu_s} \frac{\partial P_s}{\partial z}(z, t) + u \frac{\partial P_p}{\partial z}(z, t) \right. \right. \\ &\quad \left. \left. + \sum_{j=1}^J \frac{\nu_p}{\nu_j} \left(\frac{\partial P_A^+}{\partial z}(z, t, \nu_j) - \frac{\partial P_A^-}{\partial z}(z, t, \nu_j) \right) \right) \right) P_p(z, t) \end{aligned} \right. \quad (91b)$$

$$\left\{ \begin{aligned} \frac{\partial P_A^+}{\partial z}(z, t, \nu_j) &= - \left(\alpha_A^{(a)} + \frac{1}{P_A^{\text{sat}}(\nu_j)} \left(\frac{\nu_j}{\nu_s} \frac{\partial P_s}{\partial z}(z, t) + \frac{\nu_j}{\nu_p} u \frac{\partial P_p}{\partial z}(z, t) \right. \right. \\ &\quad \left. \left. + \sum_{\ell=1}^J \frac{\nu_j}{\nu_\ell} \left(\frac{\partial P_A^+}{\partial z}(z, t, \nu_\ell) - \frac{\partial P_A^-}{\partial z}(z, t, \nu_\ell) \right) \right) \right) P_A^+(z, t, \nu_j) \end{aligned} \right. \quad (91c)$$

$$\left\{ \begin{aligned} \frac{\partial P_A^-}{\partial z}(z, t, \nu_j) &= \left(\alpha_A^{(a)} + \frac{1}{P_A^{\text{sat}}(\nu_j)} \left(\frac{\nu_j}{\nu_s} \frac{\partial P_s}{\partial z}(z, t) + \frac{\nu_j}{\nu_p} u \frac{\partial P_p}{\partial z}(z, t) \right. \right. \\ &\quad \left. \left. + \sum_{\ell=1}^J \frac{\nu_j}{\nu_\ell} \left(\frac{\partial P_A^+}{\partial z}(z, t, \nu_\ell) - \frac{\partial P_A^-}{\partial z}(z, t, \nu_\ell) \right) \right) \right) P_A^-(z, t, \nu_j) \end{aligned} \right. \quad (91d)$$

Let us now divide (91a) by P_s and integrate both sides of the equation from $z = 0$ to $z = L$. We obtain in the two cases $u = \pm 1$

$$\begin{aligned} \ln \left(\frac{P_s^{\text{out}}(t)}{P_s^{\text{in}}(t)} \right) &= -\alpha_s^{(a)} L - \frac{1}{P_s^{\text{sat}}} \left(P_s^{\text{out}}(t) - P_s^{\text{in}}(t) + \frac{\nu_s}{\nu_p} (P_p^{\text{out}}(t) - P_p^{\text{in}}(t)) \right) \\ &\quad + \sum_{j=1}^J \frac{\nu_s}{\nu_j} (P_A^{+, \text{out}}(t, \nu_j) - P_A^{+, \text{in}}(t, \nu_j) + P_A^{-, \text{out}}(t, \nu_j) - P_A^{-, \text{in}}(t, \nu_j)) \end{aligned} \quad (92)$$

where $P_s^{\text{out}} = P_s(z = L)$, $P_p^{\text{out}} = P_p(z = L)$ if $u = 1$ and $P_p^{\text{out}} = P_p(z = 0)$ if $u = -1$, $P_A^{\pm, \text{out}}(\nu_j) = P_A^\pm(z = L, \nu_j)$ with similar relations for the incoming powers. Let us introduce the following energies:

$$\begin{aligned} E_s^{\text{in}} &= \nu_s^{-1} P_s^{\text{in}} & E_s^{\text{out}} &= \nu_s^{-1} P_s^{\text{out}} \\ E_p^{\text{in}} &= \nu_p^{-1} P_p^{\text{in}} & E_p^{\text{out}} &= \nu_p^{-1} P_p^{\text{out}} \\ E_A^{\text{in}}(\nu_j) &= \nu_j^{-1} (P_A^{+, \text{in}}(\nu_j) + P_A^{-, \text{in}}(\nu_j)) & E_A^{\text{out}}(\nu_j) &= \nu_j^{-1} (P_A^{+, \text{out}}(\nu_j) + P_A^{-, \text{out}}(\nu_j)) \\ E_s^{\text{sat}} &= \nu_s^{-1} P_s^{\text{sat}} & E_p^{\text{sat}} &= \nu_p^{-1} P_p^{\text{sat}} \end{aligned} \quad (93)$$

and

$$E^{\text{in}} = E_s^{\text{in}} + E_p^{\text{in}} + \sum_{j=1}^J E_A^{\text{in}}(\nu_j) \quad E^{\text{out}} = E_s^{\text{out}} + E_p^{\text{out}} + \sum_{j=1}^J E_A^{\text{out}}(\nu_j) \quad (94)$$

We deduce from (92) that

$$E_s^{\text{out}} = E_s^{\text{in}} e^{-\alpha_s^{(a)} L} e^{-\frac{E^{\text{out}} - E^{\text{in}}}{E_s^{\text{sat}}}}. \quad (95)$$

Similarly, we can divide (91b) by P_p and integrate both sides of the equation from $z = 0$ to $z = L$. This time, we obtain in the two cases $u = \pm 1$

$$E_p^{\text{out}} = E_p^{\text{in}} e^{-\alpha_p^{(a)} L} e^{-\frac{E^{\text{out}} - E^{\text{in}}}{E_p^{\text{sat}}}}. \quad (96)$$

Then, we divide (91c) by $P_A^+(\nu_j)$ and integrate both sides of the equation from $z = 0$ to $z = L$. We obtain

$$P_A^{+, \text{out}}(\nu_j) = P_A^{+, \text{in}}(\nu_j) e^{-\alpha_A^{(a)} L} e^{-\frac{E^{\text{out}} - E^{\text{in}}}{E_A^{\text{sat}}}}. \quad (97)$$

Finally, dividing (91c) by $P_A^-(\nu_j)$ and integrating both sides of the equation from $z = 0$ to $z = L$, we obtain

$$P_A^{-, \text{out}}(\nu_j) = P_A^{-, \text{in}}(\nu_j) e^{-\alpha_A^{(a)} L} e^{-\frac{E^{\text{out}} - E^{\text{in}}}{E_A^{\text{sat}}}}. \quad (98)$$

Summing (97) and (98) and dividing by ν_j , we obtain

$$E_A^{\text{out}}(\nu_j) = E_A^{\text{in}}(\nu_j) e^{-\alpha_A^{(a)} L} e^{-\frac{E^{\text{out}} - E^{\text{in}}}{E_A^{\text{sat}}}}. \quad (99)$$

To conclude, we add relations (95), (96) and (99) for all $j = 1, \dots, J$. We obtain

$$E^{\text{out}} = E_s^{\text{in}} e^{-\alpha_s^{(a)} L} e^{-\frac{E^{\text{out}} - E^{\text{in}}}{E_s^{\text{sat}}}} + E_p^{\text{in}} e^{-\alpha_p^{(a)} L} e^{-\frac{E^{\text{out}} - E^{\text{in}}}{E_p^{\text{sat}}}} + \sum_{j=1}^J E_A^{\text{in}}(\nu_j) e^{-\alpha_A^{(a)} L} e^{-\frac{E^{\text{out}} - E^{\text{in}}}{E_A^{\text{sat}}}}. \quad (100)$$

We can solve (numerically) the non-linear equation (100) to obtain the values of E^{out} for all $t \in \mathbb{R}^+$. This provides a reference case to test the accuracy of a purely numerical approach to solve the non-linear system of ODE (85).

4.3 General framework for numerical simulation

Computation of the pump, signal and ASE powers along the fiber, *i.e.* computation of $P_s(z, t)$, $P_p(z, t)$ and $P_A^\pm(z, t, \nu_j)$, $j = 1, \dots, J$, for all $z \in [0, L]$, requires the solving of the non-linear system of ODE (85). This non-linear system of ODE can not be solved analytically and a numerical approach is mandatory. This autonomous non-linear system of ODE can be expressed as

$$Y_t'(z) = -A Y_t(z) + F(Y_t(z)) \stackrel{\text{def}}{=} G(Y_t(z)) \quad (101)$$

where for any fixed $t \in \mathbb{R}^+$ the unknown function Y_t is defined as

$$Y_t : z \in [0, L] \mapsto \begin{pmatrix} P_s(z, t) \\ P_p(z, t) \\ P_A^+(z, t, \nu_1) \\ \vdots \\ P_A^+(z, t, \nu_J) \\ P_A^-(z, t, \nu_1) \\ \vdots \\ P_A^-(z, t, \nu_J) \end{pmatrix} \in \mathbb{R}^{2(J+1)}, \quad (102)$$

A denotes a diagonal matrix such that

$$A = A^{(a)} + A^{(0)} \quad (103)$$

signal and pump powers are

$$P_s(z = 0, t) = P_s^{\text{in}}(t) \quad \text{and} \quad P_p(z = 0, t) = P_p^{\text{in}}(t) \quad \forall t \in \mathbb{R}^+ \quad (107)$$

where P_s^{in} and P_p^{in} are the incoming given signal and pump powers at the fiber entry located at $z = 0$. The ASE power in the frequency sub-interval centered at the frequency ν_j is propagated as one signal with an input power of 0 at $z = 0$ for forward-propagating ASE and another signal with an input power of 0 at $z = L$ for the backward-propagating ASE. Thus the boundary conditions for the ASE powers read

$$P_A^+(z = 0, t, \nu_j) = 0 \quad \text{and} \quad P_A^-(z = L, t, \nu_j) = 0 \quad \forall t \in \mathbb{R}^+ \quad \forall j = 1, \dots, J. \quad (108)$$

In the contra-propagating case, the boundary conditions for the signal and pump powers become

$$P_s(z = 0, t) = P_s^{\text{in}}(t) \quad \text{and} \quad P_p(z = L, t) = P_p^{\text{in}}(t) \quad \forall t \in \mathbb{R}^+ \quad (109)$$

and the boundary conditions for the ASE powers remains unchanged and are given by (108).

4.4 Simulation using a Shooting method

Note that in both cases, co-propagating and contra-propagating, we do not have a Cauchy problem but a boundary value problem because of the boundary conditions for the ASE powers given by (108) at the two ends of the fiber. Thus, the non-linear ODE system (101) can be solved either by one of the *shooting methods* described in Section 3.2 and in Section 3.3. Alternatively, we can use one of the *relaxation methods* described in Section 3.4. Its implementation is however a little more tricky and we provide in the next Section some results required to implement a relaxation method for the non-linear ODE system (101).

4.5 Simulation using a Relaxation method

To solve (108) with the boundary conditions (107)–(108) (co-propagating case) or (109)–(108) (contra-propagating case), let us introduce a subdivision $(z_k)_{k=0, \dots, K}$ of the interval $[0, L]$ corresponding to the fiber. Let us consider a sub-interval $[z_k, z_{k+1}]$ for $k \in \{0, \dots, K-1\}$. We denote by $h_k = z_{k+1} - z_k$ its length and by Y_k (resp. Y_{k+1}) the approximation of Y at node z_k (resp. z_{k+1}). We can approach equation (108) in $[z_k, z_{k+1}]$ by a standard numerical scheme for an ODE system such as Runge-Kutta scheme for instance. As shown in Section 4.5, such a scheme reads

$$Y_{k+1} - Y_k - h_k \Psi(Y_k) = 0, \quad \forall k = 0, \dots, K-1 \quad (110)$$

where, when using Runge-Kutta scheme RK₂,

$$\Psi(Y_k) = G\left(Y_k + \frac{h_k}{2} G(Y_k)\right) \quad (111)$$

and when using the fourth order Runge-Kutta scheme RK₄,

$$\Psi(Y_k) = \frac{1}{6} (K_1 + 2K_2 + 2K_3 + K_4) \quad (112)$$

where

$$\begin{cases} K_1 = G(Y_k) = F(Y_k) - A Y_k \\ K_2 = G\left(Y_k + \frac{h_k}{2} K_1\right) = F\left(Y_k + \frac{h_k}{2} K_1\right) - A \left(Y_k + \frac{h_k}{2} K_1\right) \\ K_3 = G\left(Y_k + \frac{h_k}{2} K_2\right) = F\left(Y_k + \frac{h_k}{2} K_2\right) - A \left(Y_k + \frac{h_k}{2} K_2\right) \\ K_4 = G\left(Y_k + h_k K_3\right) = F\left(Y_k + h_k K_3\right) - A \left(Y_k + h_k K_3\right) \end{cases}$$

From the boundary conditions, we have in the co-propagating case ($u = 1$)

$$Y_0 = \begin{pmatrix} P_s^{\text{in}}(t) \\ P_p^{\text{in}}(t) \\ 0 \\ \vdots \\ 0 \\ Y_{0,J+3} \\ \vdots \\ Y_{0,2J+2} \end{pmatrix} \quad \text{and} \quad Y_K = \begin{pmatrix} Y_{K,1} \\ Y_{K,2} \\ Y_{K,3} \\ \vdots \\ Y_{K,J+2} \\ 0 \\ \vdots \\ 0 \end{pmatrix} \quad (113)$$

Finally, equation (47) (resp. (48)) with (70) form a non-linear system of $2(J+1)K$ equations with $2(J+1)K$ unknowns: $Y_{0,J+3}, \dots, Y_{0,2J+2}, Y_{k,1}, Y_{k,2J+2}$ for $k = \{1, \dots, K-2\}$ and $Y_{K,1}, \dots, Y_{K,J+2}$.

In the contra-propagating case ($u = -1$), we deduce from the boundary conditions

$$Y_0 = \begin{pmatrix} P_s^{\text{in}}(t) \\ Y_{0,2} \\ 0 \\ \vdots \\ 0 \\ Y_{0,J+3} \\ \vdots \\ Y_{0,2J+2} \end{pmatrix} \quad \text{and} \quad Y_K = \begin{pmatrix} Y_{K,1} \\ P_p^{\text{in}}(t) \\ Y_{K,3} \\ \vdots \\ Y_{K,J+2} \\ 0 \\ \vdots \\ 0 \end{pmatrix} \quad (114)$$

and we also have a non-linear system of $2(J+1)K$ equations with $2(J+1)K$ unknowns: $Y_{0,2}, Y_{0,J+3}, \dots, Y_{0,2J+2}, Y_{k,1}, Y_{k,2J+2}$ for $k = \{1, \dots, K-2\}$ and $Y_{K,1}, Y_{K,3}, \dots, Y_{K,J+2}$.

We will only detail in the following the co-propagating case.

In both case, when a Runge-Kutta schemes (RK_2 or RK_4) is used, we obtain the following non-linear system of equations

$$\begin{cases} Y_1 - Y_0 - h_0 \Psi(Y_0) = 0 \\ Y_{k+1} - Y_k - h_k \Psi(Y_k) = 0, \quad \forall k = 1, \dots, K-2 \\ Y_K - Y_{K-1} - h_{K-1} \Psi(Y_{K-1}) = 0 \end{cases} \quad (115)$$

We introduce as unknown $\mathbb{Y} \in \mathbb{R}^{2(J+1)K}$ such that

$$\mathbb{Y} = (Y_{0,J+3} \quad \dots \quad Y_{0,2J+2} \quad Y_{1,1} \quad \dots \quad Y_{K-1,2J+2} \quad Y_{K,1} \quad Y_{K,2} \quad Y_{K,3} \quad \dots \quad Y_{K,J+2})^\top \quad (116)$$

$$\stackrel{\text{def}}{=} (\mathbb{Y}_1 \quad \dots \quad \mathbb{Y}_{2(J+1)K})^\top$$

that is to say, for all $k = 0, \dots, K$ and for all $j = 1, \dots, J$, we have

$$Y_{k,j} = \mathbb{Y}_{2k(J+1)-(J+2)+j} \quad (117)$$

The non-linear system (116) can be recast as

$$H(\mathbb{Y}) = 0 \quad (118)$$

where the mapping $H : \mathbb{R}^{2(J+1)K} \rightarrow \mathbb{R}^{2(J+1)K}$ is defined as

$$H(\mathbb{Y}) = \begin{pmatrix} H_1(\mathbb{Y}) \\ \vdots \\ H_K(\mathbb{Y}) \end{pmatrix} \quad (119)$$

where

$$H_1(\mathbb{Y}) = \begin{pmatrix} \mathbb{Y}_{J+1} - P_s^{\text{in}} - h_0 \Psi_1(\mathbb{Y}_0) \\ \mathbb{Y}_{J+2} - P_p^{\text{in}} - h_0 \Psi_2(\mathbb{Y}_0) \\ \mathbb{Y}_{J+3} - h_0 \Psi_3(\mathbb{Y}_0) \\ \vdots \\ \mathbb{Y}_{2J+2} - h_0 \Psi_{J+2}(\mathbb{Y}_0) \\ \mathbb{Y}_{2J+3} - \mathbb{Y}_1 - h_0 \Psi_{J+3}(\mathbb{Y}_0) \\ \vdots \\ \mathbb{Y}_{3J+2} - \mathbb{Y}_J - h_0 \Psi_{2J+2}(\mathbb{Y}_0) \end{pmatrix}$$

with $\mathbb{Y}_0 = (P_s^{\text{in}}, P_p^{\text{in}}, 0, \dots, 0, \mathbb{Y}_1, \dots, \mathbb{Y}_J)^\top$ and, for $k = 1, \dots, K-2$,

$$H_{k+1}(\mathbb{Y}) = \left(\mathbb{Y}_{2k(J+1)+J+j} - \mathbb{Y}_{2k(J+1)-(J+2)+j} - h_k \Psi_j(\mathbb{Y}_k) \right)_{j=1, \dots, J}$$

with $\mathbb{Y}_k = (\mathbb{Y}_{2k(J+1)-J-1}, \dots, \mathbb{Y}_{2k(J+1)+J})^\top$ and

$$H_K(\mathbb{Y}) = \begin{pmatrix} \mathbb{Y}_{2(K-1)(J+1)+J+1} - \mathbb{Y}_{2(K-1)(J+1)-(J+1)} - h_{K-1} \Psi_1(\mathbb{Y}_{K-1}) \\ \vdots \\ \mathbb{Y}_{2K-(J+1)} - \mathbb{Y}_{2(K-1)(J+1)-1} - h_{K-1} \Psi_{J+2}(\mathbb{Y}_{K-1}) \\ - \mathbb{Y}_{2(K-1)(J+1)} - h_{K-1} \Psi_{J+3}(\mathbb{Y}_{K-1}) \\ \vdots \\ - \mathbb{Y}_{2(K-1)(J+1)+J} - h_{K-1} \Psi_{2J+2}(\mathbb{Y}_{K-1}) \end{pmatrix}$$

with $\mathbb{Y}_{K-1} = (\mathbb{Y}_{2(K-1)(J+1)-J-1}, \dots, \mathbb{Y}_{2(K-1)(J+1)+J})^\top$.

The expressions of the Ψ_j depend on the choice made for *Method A* in the relaxation approach. For instance, when using the RK2 scheme, we have for $\mathbb{X} = (X_1, \dots, X_{2J+2}) \in \mathbb{R}^{2J+2}$

$$\Psi_i(\mathbb{X}) = G_i(\mathbb{X} + \frac{h_k}{2} G(\mathbb{X})) \quad i = 1, \dots, 2J+2 \quad (120)$$

where G_i denotes the i -th component of the mapping G defined in (101).

The more natural choice for a numerical method for solving the non-linear system (118) is Newton-Raphson method. Starting from an initial guess $\mathbb{Y}^{(0)} \in \mathbb{R}^{2K(J+1)}$, Newton-Raphson method defines a sequence $(\mathbb{Y}^{(n)})_{n \in \mathbb{N}}$ such that

$$\mathbb{Y}^{(n)} = \mathbb{Y}^{(n-1)} + \delta^{(n-1)} \quad \forall n \geq 1 \quad (121)$$

where $\delta^{(n)}$ denotes the solution to the linear system

$$\mathbf{J}_H(\mathbb{Y}^{(n-1)}) \delta^{(n-1)} = -H(\mathbb{Y}^{(n-1)}) \quad (122)$$

where $\mathbf{J}_H(\mathbb{Y}^{(n-1)})$ is the Jacobian matrix of the mapping H evaluated in $\mathbb{Y}^{(n-1)}$, that is to say

$$\mathbf{J}_H(\mathbb{Y}^{(n-1)}) = \begin{pmatrix} \partial_1 H_1(\mathbb{Y}^{(n-1)}) & \dots & \partial_{2(J+1)K} H_1(\mathbb{Y}^{(n-1)}) \\ \vdots & & \vdots \\ \partial_1 H_{2(J+1)K}(\mathbb{Y}^{(n-1)}) & \dots & \partial_{2(J+1)K} H_{2(J+1)K}(\mathbb{Y}^{(n-1)}) \end{pmatrix} \quad (123)$$

Because of the expression of the mapping H in this study, see (119) and the expressions below, the matrix J_H is sparse and it has the following block expression in $\mathbb{Y} \in \mathbb{R}^{2K(J+1)}$

$$J_H(\mathbb{Y}) = \begin{pmatrix} D_0 & I_{2J+2} & & & & \\ & D_1 & I_{2J+2} & & & \\ & & D_2 & I_{2J+2} & & \\ & & & \ddots & \ddots & \\ & & & & D_{K-2} & I_{2J+2} \\ & & & & & D_{K-1} & \tilde{\mathbf{I}} \end{pmatrix} \quad (124)$$

where the blocks not represented out of the two diagonals are all zeros, I_{2J+2} denotes the identity matrix in $\mathcal{M}_{2J+2}(\mathbb{R})$ and for $k = 1, \dots, K-1$

$$D_k = -I_{2J+2} - h_k J_\Psi(\mathbf{Y}_k)$$

where $\mathbf{Y}_k = (\mathbb{Y}_{2k(J+1)-J-1}, \dots, \mathbb{Y}_{2k(J+1)+J})^\top$ and

$$\tilde{\mathbf{I}} = \begin{pmatrix} I_{J+2} \\ O \end{pmatrix} \in \mathcal{M}_{2J+2, J+2}(\mathbb{R})$$

$$D_0 = - \begin{pmatrix} O \\ I_J \end{pmatrix} - h_0 \begin{pmatrix} \partial_{J+3} \Psi_1(\mathbf{Y}_0) & \dots & \partial_{2J+2} \Psi_1(\mathbf{Y}_0) \\ \vdots & & \vdots \\ \partial_{J+3} \Psi_{2J+2}(\mathbf{Y}_0) & \dots & \partial_{2J+2} \Psi_{2J+2}(\mathbf{Y}_0) \end{pmatrix}$$

where $\mathbf{Y}_0 = (P_s^{\text{in}}, P_p^{\text{in}}, 0, \dots, 0, \mathbb{Y}_1, \dots, \mathbb{Y}_J)$.

It remains to express the Jacobian matrix of Ψ . We only consider the case of a RK2 scheme where Ψ is expressed in (120). From the chain rule, we obtain

$$J_\Psi(\mathbf{Y}_k) = J_G(\mathbf{Y}_k + \frac{h_k}{2} G(\mathbf{Y}_k)) \times \left(I_{2J+2} + \frac{h_k}{2} J_G(\mathbf{Y}_k) \right) \quad (125)$$

and we have

$$J_G(\mathbf{Y}_k) = -\mathbf{A} + J_F(\mathbf{Y}_k) \quad (126)$$

where the matrix \mathbf{A} is defined in (103). To conclude this computation, we have to express the Jacobian of F where F is given in (104). For all $\mathbf{Y} = (Y_1, \dots, Y_{2J+2})^\top \in \mathbb{R}^{2J+2}$, we can express $F(\mathbf{Y})$ as

$$F(\mathbf{Y}) = \begin{pmatrix} \frac{g_s(\mathbf{Y})}{d(\mathbf{Y})} \frac{Y_1}{P_s^{\text{sat}}} \\ u \frac{g_p(\mathbf{Y})}{d(\mathbf{Y})} \frac{Y_2}{P_p^{\text{sat}}} \\ \frac{\Gamma_1}{\Gamma_s} \frac{g_1(\mathbf{Y})}{d(\mathbf{Y})} \left(\frac{Y_3}{P_A^{\text{sat}}(\nu_1)} + \frac{1}{2} \frac{P_A^{(0)}(\nu_1)}{P_A^{\text{sat},(e)}(\nu_1)} \right) \\ \vdots \\ \frac{\Gamma_J}{\Gamma_s} \frac{g_J(\mathbf{Y})}{d(\mathbf{Y})} \left(\frac{Y_{J+2}}{P_A^{\text{sat}}(\nu_J)} + \frac{1}{2} \frac{P_A^{(0)}(\nu_J)}{P_A^{\text{sat},(e)}(\nu_J)} \right) \\ - \frac{\Gamma_1}{\Gamma_s} \frac{g_1(\mathbf{Y})}{d(\mathbf{Y})} \left(\frac{Y_3}{P_A^{\text{sat}}(\nu_1)} + \frac{1}{2} \frac{P_A^{(0)}(\nu_1)}{P_A^{\text{sat},(e)}(\nu_1)} \right) \\ \vdots \\ - \frac{\Gamma_J}{\Gamma_s} \frac{g_J(\mathbf{Y})}{d(\mathbf{Y})} \left(\frac{Y_{J+2}}{P_A^{\text{sat}}(\nu_J)} + \frac{1}{2} \frac{P_A^{(0)}(\nu_J)}{P_A^{\text{sat},(e)}(\nu_J)} \right) \end{pmatrix} \quad (127)$$

where

$$d(\mathbf{Y}) = 1 + \frac{Y_1}{P_s^{\text{sat}}} + \frac{Y_2}{P_p^{\text{sat}}} + \sum_{k=1}^J \frac{Y_{2+k} + Y_{2+J+k}}{P_A^{\text{sat}}(\nu_k)}$$

and

$$\begin{aligned}
g_s(\mathbf{Y}) &= \alpha_s^{(a)} Y_1 + \frac{\nu_s}{\nu_p} \alpha_p^{(a)} Y_2 + \sum_{k=1}^J \frac{\nu_s}{\nu_k} \alpha_A^{(a)}(\nu_k) (Y_{2+k} + Y_{2+J+k}) \\
g_p(\mathbf{Y}) &= \frac{\nu_p}{\nu_s} \alpha_s^{(a)} Y_1 + \alpha_p^{(a)} Y_2 + \sum_{k=1}^J \frac{\nu_p}{\nu_k} \alpha_A^{(a)}(\nu_k) (Y_{2+k} + Y_{2+J+k}) \\
g_j(\mathbf{Y}) &= \frac{\nu_j}{\nu_s} \alpha_s^{(a)} Y_1 + \frac{\nu_j}{\nu_p} \alpha_p^{(a)} Y_2 + \sum_{k=1}^J \frac{\nu_j}{\nu_k} \alpha_A^{(a)}(\nu_k) (Y_{2+k} + Y_{2+J+k})
\end{aligned}$$

For all $\mathbf{Y} = (Y_1, \dots, Y_{2J+2})^\top \in \mathbb{R}^{2J+2}$, the Jacobian of F in \mathbf{Y} can be expressed as

$$J_F(\mathbf{Y}) = \frac{1}{d(\mathbf{Y})} \mathbf{M}_1 + \mathbf{M}_2 \times \mathbf{M}_3 \quad (128)$$

where $\mathbf{M}_1 \in \mathcal{M}_{2J+2}(\mathbb{R})$ is a diagonal matrix with diagonal entries

$$\left(\frac{g_s(\mathbf{Y})}{P_s^{\text{sat}}}, \frac{u g_p(\mathbf{Y})}{P_p^{\text{sat}}}, \frac{\Gamma_1}{\Gamma_s} \frac{g_1(\mathbf{Y})}{P_A^{\text{sat}}(\nu_1)}, \dots, \frac{\Gamma_J}{\Gamma_s} \frac{g_J(\mathbf{Y})}{P_A^{\text{sat}}(\nu_J)}, -\frac{\Gamma_1}{\Gamma_s} \frac{g_1(\mathbf{Y})}{P_s^{\text{sat}}(\nu_1)}, \dots, -\frac{\Gamma_J}{\Gamma_s} \frac{g_J(\mathbf{Y})}{P_s^{\text{sat}}(\nu_J)} \right) \quad (129)$$

$\mathbf{M}_2 \in \mathcal{M}_{2J+2}(\mathbb{R})$ is a diagonal matrix with diagonal entries

$$\left(\frac{Y_1}{P_s^{\text{sat}}}, \frac{u Y_2}{P_p^{\text{sat}}}, \frac{\Gamma_1}{\Gamma_s} \frac{Y_3}{P_A^{\text{sat}}(\nu_1)}, \dots, \frac{\Gamma_J}{\Gamma_s} \frac{Y_{J+2}}{P_A^{\text{sat}}(\nu_J)}, -\frac{\Gamma_1}{\Gamma_s} \frac{Y_{3+J}}{P_s^{\text{sat}}(\nu_1)}, \dots, -\frac{\Gamma_J}{\Gamma_s} \frac{Y_{2J+2}}{P_s^{\text{sat}}(\nu_J)} \right) \quad (130)$$

and

$$\mathbf{M}_3 = \frac{1}{d(\mathbf{Y})} \mathbf{M}_{3,1} - \frac{1}{d^2(\mathbf{Y})} \mathbf{M}_{3,2} \quad (131)$$

where $\mathbf{M}_{3,1}$ and $\mathbf{M}_{3,2}$ are the matrix of $\mathcal{M}_{2J+2}(\mathbb{R})$ defined as the following matrix product of a column matrix by a row matrix

$$\begin{aligned}
\mathbf{M}_{3,1} &= \begin{pmatrix} \nu_s \\ \nu_p \\ \nu_1 \\ \vdots \\ \nu_J \\ \nu_1 \\ \vdots \\ \nu_J \end{pmatrix} \times \begin{pmatrix} \alpha_s^{(a)} & \alpha_p^{(a)} & \alpha_A^{(a)}(\nu_1) & \dots & \alpha_A^{(a)}(\nu_J) & \alpha_A^{(a)}(\nu_1) & \dots & \alpha_A^{(a)}(\nu_J) \\ \nu_s & \nu_p & \nu_1 & & \nu_J & \nu_1 & & \nu_J \end{pmatrix} \\
\mathbf{M}_{3,2} &= \begin{pmatrix} g_s(\mathbf{Y}) \\ g_p(\mathbf{Y}) \\ g_1(\mathbf{Y}) \\ \vdots \\ g_J(\mathbf{Y}) \\ g_1(\mathbf{Y}) \\ \vdots \\ g_J(\mathbf{Y}) \end{pmatrix} \times (\partial_1 d(\mathbf{Y}) \quad \dots \quad \partial_{2J+2} d(\mathbf{Y}))
\end{aligned}$$

Note that we have

$$\partial_j d(\mathbf{Y}) = \begin{cases} \frac{1}{P_s^{\text{sat}}} & \text{if } j = 1 \\ \frac{1}{P_p^{\text{sat}}} & \text{if } j = 2 \\ \frac{1}{P_A^{\text{sat}}(\nu_{j-2})} & \text{if } j \in \{3, \dots, J+2\} \\ \frac{1}{P_A^{\text{sat}}(\nu_{j-2-J})} & \text{if } j \in \{J+3, \dots, 2J+2\} \end{cases}$$

4.6 Numerical experiments

We have considered a Erbium fiber amplifier with the following properties:

- Fiber length $L = 2$ m
- Erbium ions density $N = 1.4 \cdot 10^{25} \text{ m}^{-3}$
- $\lambda_s = 1.55 \cdot 10^{-6} \text{ m}$
- $\lambda_p = 0.976 \cdot 10^{-6} \text{ m}$
- $\Gamma_p = 0.785$
- $\Gamma_s = 0.43$
- $A_{\text{eff}} = 5.64 \cdot 10^{-12} \text{ m}^2$
- $\alpha_p^{(a)} = 1.3816 \cdot 10^{-3} \text{ m}^{-1}$
- $\alpha_s^{(a)} = 1.3816 \cdot 10^{-3} \text{ m}^{-1}$
- $\alpha_p^{(0)} = 0 \text{ m}^{-1}$
- $\alpha_s^{(0)} = 0 \text{ m}^{-1}$
- Metastable level 2 lifetime $\tau_2 = 10^{-2} \text{ s}$
- $\sigma_p^{(a)} = 2.1841 \cdot 10^{-25} \text{ m}^2$
- $\sigma_p^{(e)} = 0 \text{ m}^2$
- $\sigma_s^{(a)} = 2.6656 \cdot 10^{-25} \text{ m}^2$
- $\sigma_s^{(e)} = 3.9178 \cdot 10^{-25} \text{ m}^2$
- $P_s^{\text{in}} = 10^{-7} \text{ W}$
- $P_p^{\text{in}} = 8 \cdot 10^{-2} \text{ W}$

The amplified spontaneous emission (ASE) phenomenon, its features are as follows. The spectral bandwidth for the ASE ranges from 1.52 to 1.58 μm . The variations of the absorption and emission cross sections along the wavelength bandwidth of interest, obtained from experimental data, are depicted in Fig. 6. The spectral resolution was set to 0.4 nm, that is to say we have $J = 150$.

4.6.1 Simulation by the Shooting method

We first provide results obtained by the Shooting method variant described in Section 3.3. The Cauchy problem at each iteration of the Shooting method is solved by MATLAB `ode45` solver with a tolerance set to 10^{-6} . The stopping criterium for the Shooting method is that

$$\left(\sum_{j=1}^J (P_A^-(\nu_j, z = L))^2 \right)^{\frac{1}{2}} \leq \tau_s$$

where the tolerance τ_s was set to 10^{-8} . (We recall that the boundary condition at the fiber end ($z = L$) reads $P_A^-(\nu_j, z = L) = 0$ for all $j = 1, \dots, J$.)

When we assume a noise power such that $P_A^{(0)}(\nu_j) = 0$ in order to be in the situation where we have obtained the analytical expression of the total power leaving the fiber in Section 4.2, we obtain the following results.

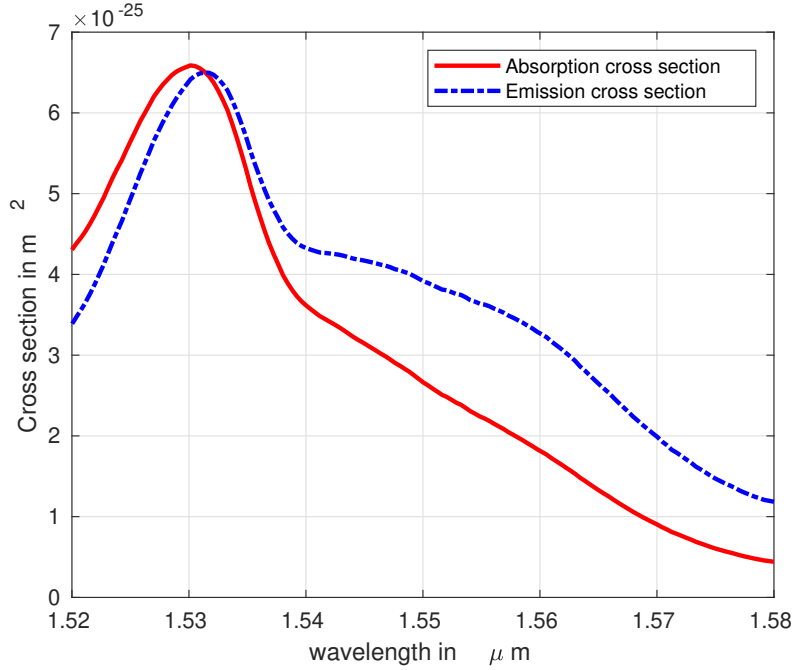


Figure 6: Variations of the absorption and emission cross sections (in m^2) along the wavelength bandwidth of interest.

CPU Time = 0.32 s.

Number of iterations = 5

Comparison of the value of the total power out :

By solving the nonlinear ODE system $P_{\text{out}} = 0.076333$

By solving the nonlinear equ. $P_{\text{out}} = 0.076333$

Relative error = $8.537\text{e-}11$

This validates the computer program: the relative error in this special case is around 10^{-10} .

We then simulate light-wave propagation in the amplifier under the assumption that the noise power is given by (74). CPU time is then 0.22 s. and the Shooting method converges to the prescribed tolerance in 5 iterations. We have depicted in Fig. 7 the variations of the pump, source and total ASE powers along the fiber and the variations of the forward and backward ASE powers in log scale (dbm) as a function of the wavelength.

4.6.2 Simulation by the Relaxation method

We provide in this Section results obtained by the Relaxation method described in Section 3.4. We have used a Runge-Kutta RK2 scheme for method A and the Newton-Raphson method (method B) to solve the non-linear system. In the Newton-Raphson method, the Jacobian matrix is handled in MATLAB *sparse* form and the `mldivide` command is used to solve the linear system at each iteration of the Newton-Raphson algorithm.

When we assume a noise power such that $P_A^{(0)}(\nu_j) = 0$ in order to be in the situation where we have obtained the analytical expression of the total power leaving the fiber in Section 4.2, we obtain the following results.

CPU time of the simulation = 22.47 s.

Number of iteration of Newton-Raphson method = 14

Comparison of the value of the total power out :

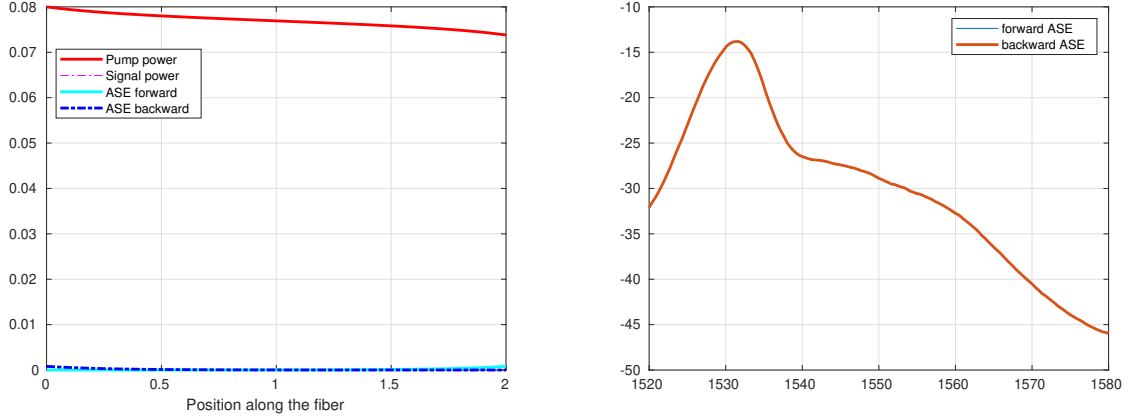


Figure 7: Variations of the pump, source and total ASE powers along the fiber (left) and variations of the forward and backward ASE powers in log scale (dbm) as a function of the wavelength (right).

```
By solving the nonlinear ODE systeme P_out = 0.076333
By solving the nonlinear equ. P_out = 0.076333
Relative error = 9.3097e-09
```

This validates the computer program: the relative error in this special case is around 10^{-8} . Note that the computation time is much higher than the computation time of the Shooting method variant.

We then simulate light-wave propagation in the amplifier under the assumption that the noise power is given by (74). CPU time is then 207 s. and the Relaxation method converges to the prescribed tolerance in 20 iterations. The result obtained for the variations of the pump, source and total ASE powers along the fiber and the variations of the forward and backward ASE powers in log scale (dbm) as a function of the wavelength are identical to the ones obtained by the Shooting method and depicted in Fig. 7.

Acknowledgments

The author would like to sincerely thanks Arnaud Fernandez from the Laboratory for Analysis and Architecture of Systems (LAAS) in Toulouse (France) and Laurent Provino from Photonics Bretagne in Lannion (France) for the numerous fruitful discussions on EDFA..

References

- [1] P. BECKER, A. OLSSON, AND J. SIMPSON, *Erbium-Doped Fiber Amplifiers: Fundamentals and Technology*, Optics and Photonics, Elsevier Science, 1999.
- [2] E. DESURVIRE, *Erbium-Doped Fiber Amplifiers: Principles and Applications*, Wiley Series in Telecommunications and Signal Processing, Wiley, 2002.
- [3] C. R. GILES AND E. DESURVIRE, *Modeling erbium-doped fiber amplifiers*, Journal of Light-wave Technology, 9 (1991), pp. 271–283.